Investigation of RCA aptamer-based microfluidic system for *E. coli* O157:H7 detection

Shuying Li

A thesis submitted to the Faculty of Graduate and Postdoctoral Studies

in partial fulfillment of the requirements for the degree of

MASTER OF APPLIED SCIENCE

in Biomedical Engineering

Ottawa-Carleton Institute of Biomedical Engineering

University of Ottawa

Ottawa, Canada

January 2020

Abstract

Aptamers have been widely used as capturing agents to improve the sensitivity and specificity of microfluidic detection systems. This study uses rolling circle amplification (RCA) to produce repeating capturing aptamers or capturing RCA (cRCA) aptamers. The *in situ* cRCA reaction is carried out on the inner surfaces of microchannel to generate a long single-stranded DNA molecule containing tandem repeating cRCA aptamers that are specific for *E. coli* O157:H7 cells recognition. While optimizing the capturing performance of the cRCA aptamer-based microfluidic detection system, we find that the best capturing performance is achieved when the *in situ* cRCA reaction is carried out for 2 hours in order to modify the microchannel. In addition, the cRCA products are characterized using water contact angle measurement, fluorescence test, real-time quantitative PCR analysis, and atomic force microscopy (AFM). Furthermore, in order to test the sensitivity of the optimized detection system, the cRCA aptamer modified microchannel is used to detect iced tea and bottled water samples doped with *E. coli* O157:H7 cells. Our results show that the detection sensitivity and the capturing performance of this optimized cRCA aptamer detection system are about 10 times that of the conventional unit aptamer modified microfluidic detection system. In addition, our results also show that the cRCA aptamer approach had consistently higher target capturing efficiency at higher flow rates, suggesting its potential applications in sensitive detections under high throughput conditions.

Résumé

Les aptamères ont été largement utilisé comme agents de capture pour améliorer la sensibilité et la spécificité du système de détection microfluidique. Cette étude utilise l'amplification en cercle roulant (RCA) pour produire des aptamères à capture répétée ou des aptamères à RCA (cRCA). La réaction cRCA in situ est effectuée à la surface d'un microcanal pour générer une longue molécule d'ADN monocaténaire contenant des aptamères cRCA répétés en tandem qui sont spécifiques de la reconnaissance des cellules *E. coli* O157:H7. En optimisant la performance de capture du système de détection microfluidique à base d'aptamère cRCA, nous constatons que la meilleure performance de capture est atteinte lorsque la réaction cRCA in situ est effectuée pendant 2 heures afin de modifier le microcanal. De plus, les produits cRCA sont caractérisés en utilisant la mesure de l'angle de contact avec l'eau, le test de fluorescence, l'analyse quantitative PCR en temps réel et la microscopie à force atomique (AFM). Aussi, afin de tester la sensibilité du système de détection optimisé, le microcanal modifié par aptamères cRCA est utilisé pour détecter les échantillons de thé glacé et d'eau en bouteille contaminés par des cellules *E. coli* O157:H7. Nos résultats montrent que la sensibilité de détection et la performance de capture de ce système de détection d'aptamère optimisé sont environ 10 fois supérieures à celles du système de détection microfluidique modifié par aptamère de l'unité classique. De plus, nos résultats montrent également que l'approche aptamère cRCA a toujours eu une cible plus élevée pour capturer

l'efficacité à des débits plus élevés, ce qui suggère ses applications potentielles dans les détections sensibles dans des conditions de cadence élevée.

Acknowledgements

First and foremost, I would like to express my sincere gratitude to my supervisors Dr. Xudong Cao and Dr. Shan Zou for offering me valuable opportunities to join their groups in University of Ottawa and National Research Council Canada, respectively. I also appreciate their patience, enthusiastic encouragement and constructive suggestion to continuously help me in all the time of research and writing of this thesis. I could not have imagined having a better mentor and advisor for my graduate study and life.

My praises and acknowledgement also go to professors and faculty members in our department for providing academic services and technical supports. Many thanks to Dr. Jean-Philip St-Pierre and Dr. Marianne Fenech for generously sharing their laboratories and instruments. I also wish to thank colleagues in National Research Council. I thank Dr. Maohui Chen and Dr. Zygmunt Jakubek for the technical consultations and instrument training. I also would like to acknowledge Dr. Min Lin for providing bacterial samples.

I would like to extend my thanks to my colleague and many friends in the department. I thank Yuqian Jiang and Yubo Qin for their friendship and instruction to my research work. I also would like to acknowledge my colleague Jordan Nhan for his participation to this project. I feel lucky and grateful to have other colleagues and friends during my graduate study and they are Danni

Zou, Hesham Elkhadem, Holly McCulloch, Taisa Stumpf, Tongda Li, Xingkai Hao and Zhong Wang.

Finally, my sincere thanks go to my dear family members for their eternal love and support. Special thank to Ms. Xian Piao for her help, companionship and encouragement.

Table of Contents

List of Figures

List of Tables

List of Abbreviations

AFM	Atomic force microscopy
ANOVA	Analysis of variance
APTMS	(3-Aminopropyl)trimethoxysilane
APTES	(3-Aminopropyl)triethoxysilane
CAD	Computer-aided design
CDC	Centers for Disease Control and Prevention
CFU	Colony-forming unit
cRCA	Rolling circle amplification for capturing target
CT-SMAC	Cefixime potassium tellurite sorbitol-MacConkey agar
Cy3	Cyanine 3
Cy5	Cyanine 5
DNA	Deoxyribonucleic acid
dNTP	Deoxynucleotide triphosphate
DCT	Direct-charge transfer
DTT	Dithiothreitol

dsDNA	Double stranded deoxyribonucleic acid
E. coli	*Escherichia coli*
EDC	1-ethyl-3-(3-dimethylaminopropyl) carbodiimide hydrochloride
EDTA	Ethylenediaminetetraacetic acid
ELISA	Enzyme-linked immunosorbent assay
FBA	Fluorescent bacteriophage assay
FDA	Food and Drug Administration
FITC	Fluorescein isothiocyanate
HUS	Hemolytic uremic syndrome
LRSP-FS	Long-range surface plasmon-enhanced fluorescence spectroscopy
LOD	Limit of detection
MES	2-(4-morpholino)-ethane sulfonic acid
MEMS	Micro-Electro-Mechanical Systems
NHS	N-Hydroxysuccinimide
NSAID	Nonsteroidal anti-inflammatory drug
PAMAM	Poly(amidoamine)

PBS	Phosphate buffered saline
PCR	Polymerase chain reaction
PDGF	Platelet-derived growth factor
PDMS	Polydimethylsiloxane
PEG	Polyethylene glycol
PSA	Prostate specific antigen
RCA	Rolling circle amplification
RT	Room temperature
RNA	Ribonucleic acid
SELEX	Systematic evolution of ligands by exponential enrichment
SMAC	Sorbitol-MacConkey
SNP	Single nucleotide polymorphism
SPR	Surface plasmon resonance
sRCA	Rolling circle amplification for signal intensification
ssDNA	Single stranded deoxyribonucleic acid
SWNT	Single-wall carbon nanotube

UV	Ultraviolet
VEGF	Vascular endothelial growth factor
WG-RCA	Whole genome amplification *via* rolling-circle amplification
μTAS	Micro total analysis systems

Chapter 1. Introduction

Foodborne pathogenic bacteria pose a significant challenge to food safety and public health. For example, *E. coli* O157:H7 bacteria is one of the most common pathogenic bacteria that are known to cause food and water poisoning [1]. It is estimated there were 73,000 cases of infections in the US annually caused by *E. coli* O157:H7, according to the US Centers for Disease Control and Prevention (CDC) [2]. In Canada, there were 29 confirmed cases of illness caused by *E. coli* O157:H7 contaminated romaine lettuce in 2018, according to the Public Health Agency of Canada [3]. As a result, there is a pressing need to find a detection method of pathogenic bacteria in their initial growth stages in various food and drinking samples for alleviating the foutbreaks. Conventional cell plating techniques are very sensitive, but require several days and trivial steps to pre-enrich samples and they are unable to analyze new bacteria. [4, 5]. Alternatively, immunological methods such as enzyme-linked immunosorbent assay (ELISA) are commonly used in detection applications, but have been shown to be significantly less sensitive with a limit of detection (LOD) of 10^3-10^4 CFU/mL, which is not suitable for the targets with very low infectious doses [6]. Meanwhile, molecular biology based methods such as polymerase chain reaction (PCR) can quickly detect bacteria with high specificity, but requires complex sample processing steps, such as sample purifications and gene extractions [7]. Therefore, there is an urgent demand for a much more effective and sensitive method for integrating the whole cell detection, bypassing sample enrichment and separation [8]. To this end, lab-on-chip techniques

have been used as a rapid and cost-effective technique for pathogen detections [9]. In the past decade, there has been increasing attention to applying microfluidic systems to the pathogen detection [10, 11]. For instance, microfluidic devices have been used to detect *E. coli* O157:H7 with good sensitivity and specificity [12, 13]. The introduction of microfluidic to the detection system helps to minimize the size of devices which requires very few samples and reagents. Due to the small size of components, the sensitivity of detection is greatly enhanced while the LOD is lowered. However, the microfluidic devices fail to effectively capture the majority of the cells under increased flow rate, which is a well recognized deficiency in rapid and sensitive detection using microfluidic devices [14]. Therefore, there is a real need to improve the detection performance of these microfluidic devices [14-17].

Rolling circle amplification (RCA) is an isothermal DNA amplification technique that utilizes a circular, single-stranded DNA template and a DNA polymerase with strand-displacement activities. The whole process starts with the formation of a circular template, synthesized by ligating a linear DNA template and primer. Subsequently, the DNA polymerase initiates DNA elongation by adding the dNTPs to the 3' end of the primer in order to produce a long, single-stranded DNA product overtime. The RCA reactions can be carried out at mild reaction temperature, which are much easier to be perform in a natural environment as compared to PCR requiring a wide range of temperatures for thermocycling [18]. Recently, RCA reactions have been increasingly used as a method for sensitive detection. For example, RCA has been used to amplify the signal to increase the sensitivity of detection towards nucleic acids, proteins, and pathogens

[19-22]. In our previous study, RCA has been used in an aptamer-based microfluidic detection system for signal amplification (coded as sRCA). The sRCA products are long single-stranded DNA chains containing multiple binding sites for complementary fluorescence probes, further enhancing the signal intensity by 30-40 fold to achieve decreased the limit of detection (LOD) from 10^3 to 10^2 cells/mL [23].

In the current study, in order to improve the capturing performance of aptamer-based microfluidic detection system in the detection of liquid samples, RCA process was used to produce polyvalent capturing aptamer for target bacteria, which is called capturing RCA, or cRCA.

The overall goal of this study is to develop a rapid and sensitive cRCA aptamer-based microfluidic device for *E. coli* O157:H7 detection in liquid samples. To achieve this goal, there are the following objectives will be carried out:

(1) To prepare a cRCA aptamer modified microchannel using PAMAM dendrimers as templates for subsequent *in situ* cRCA reactions [24].

(2) To confirm the success of the *in situ* cRCA process on the surface of the microchannel.

(3) To investigate optimal conditions of cRCA reaction time and flow rate of sample injection for most effective capturing performance and higher throughput for detecting target *E. coli* O157:H7 cells.

(4) To test the capturing performance of this cRCA aptamer-based microfluidic detection system in the real-world application of detecting the target *E. coli* O157:H7 cells in the spiked PBS solution, iced tea and bottled water.

The results of experiments showed the optimal condition for the microchannel is using 2 h cRCA aptamer to capture target cells with a flow rate of 0.5 mL/h. In addition, the throughput of the optimal microfluidic detection system with cRCA aptamer increased 10-fold, while the sensitivity was enhanced more than 10-fold, as compared to our previous detection system. In addition, this study discovered a phenomenon that the capturing performance of cRCA aptamer did not keep increasing with time. Furthermore, according to the analysis of the atomic force microscopy (AFM) characterization of cRCA products and the fluorescence test of these cRCA modified PDMS surfaces, it was suggested that there were increasing extra double-stranded DNA structures produced after the cRCA process reached 3 h, which cut down the amount of capturing structures in the extended cRCA products.

Chapter 2. Literature review

2.1 Methods for *Escherichia. coli* O157:H7 (*E. coli* O157:H7) detection

E. coli O157:H7 is one of the most common and serious pathogens [25]. It is the most frequently isolated serotype of the Shiga toxin-producing *E. coli*. As a result, people who are infected show symptoms such as acute hemorrhagic diarrhea, abdominal cramps and even hemolytic uremic syndrome (HUS) for some vulnerable populations such as young children or the elderly [26]. The most common method of transmission for *E. coli* O157:H7 infections is through contaminated food and water, and it can be spread from person to person and from animal to person [2]. It has been established that most outbreaks occur after the ingestion of contaminated food since the pathogen can stay alive during food processing procedures, and even survive the process of cooking [27]. It is also important to note that *E. coli* O157:H7 has a very low infectious dose of 10-10^2 CFU, compared to over 10^6 CFU for other *E. coli* strains [28, 29].

With the development of biotechnology, there are many emerging methods for improving the detection efficiency. Several common methods are listed in Table 1, and their LOD, process time and specificity are also tabulated. Conventional methods include cell plating, cell culture, and biochemical tests. These methods are very sensitive and accurate for target detections, but they need several days to complete and require a time-consuming cell enrichment step and laborious sample preparation procedures [30-32]. Immunological methods such as enzyme-linked immunosorbent assay (ELISA) have also been used as a rapid and sensitive detection method. For

instance, a sandwich ELISA method was used to detect *E. coli* O157:H7 cells. In this case, an anti-*E. coli* O157:H7 IgY was used as the capturing antibody while a biotinylated mouse monoclonal antibody was used as the secondary antibody. After subsequent incubation of streptavidin-HRPO and further interaction with TMB substrate, the results can be obtained from an ELISA microplate reader. The LOD of this method was reported as 40 CFU/mL [33]. This method is sensitive butdoes not claim its specificity result.. Molecular biology methods such as polymerase chain reaction (PCR) can also identify bacteria with high specificity, through the use of oligonucleotide probes known as primers, which complementarily base pairing with their target genes [7]. For example, a PCR-acoustic wave sensor was used to detect specific target sequences of *E. coli* O157:H7. They used PCR to amplify the sequence unique to the target cell, meanwhile a biotinylated probe was attached to the surface of the sensor *via* the biotin-neutravidin interaction to detect the hybridization of the sequence with sample [34]. This method was suggested to rapidly test the real sample; however, this method requires laborious sample concentration and gene extraction procedure.

Table 1. Features of common methods used for pathogen detection.

Method	**LOD (CFU/mL)**	**Detection time**	**Specificity**	**Reference**
Plate culture	1	1-3 days	Good	[35, 36]
ELISA	10^4	1-2 days	Good	[37, 38]
Flow cytometry	10^2-10^3	0.5 h	Good	[39, 40]
PCR	1	16-24 h	Good	[41, 42]
Fiber optic biosensor	10^3	24 h	NA	[43, 44]
Bioluminescent biosensor	10^4	0.5 h	NA	[45, 46]
Aptamer-based biosensor	10-10^2	6-12 h	Excellent	[47, 48]
Antibody-SPR based biosensor	10^2-10^3	0.5 h	Good	[49, 50]

Note: The specificity was classified into "Excellent" for 100% specificity, "Good" for reported good specificity but without accurate value of specificity and "NA" for that no mention.

Biosensors are becoming more common devices for bacteria detections since it offers the rapid and effective detection at the point-of-care. There are increasing research efforts focusing on developing various biosensors for whole bacteria detection. For example, Demarco *et al*. developed a portable fiber-optic biosensor to detect *E. coli* O157:H7 cells in ground beef samples. They used a sandwich immunoassay with Cy5 labeled polyclonal anti-*E. coli* O157:H7 antibodies.

Next, light was launched from a 635-nm diode laser into a dual tapered 600-µm silica fiber. Then, the fiber surface was excited by the evanescent field, and part of the emission was recoupled into the fiber, while a photodiode was used to detect the fluorescent signals. This biosensor reported the LOD with 3-30 CFU/mL in ground beef sample [43]. In addition, the technique of surface plasmon resonance (SPR) has been used as an optical biosensor. The first SPR instrument was developed in 1990, called Biacore. The objective is to detect changes in the dielectric constant when an antigen binds to an antibody immobilized onto the gold or silver surface. The detection was fast and in real-time as long as the immunochemical reaction takes place [51]. Fratamico *et al*. studied a Biacore biosensor utilizing antibodies against *E. coli* O157:H7 cell to have a LOD of 5×10^7 CFU/mL. However, it was far from meeting the requirement of sensitivity for detecting *E. coli* O157:H7 cells. Huang *et al.* designed a biosensor system based on long-range surface plasmon-enhanced fluorescence spectroscopy (LRSP-FS) to detect *E. coli* O157:H7 cells. The purpose was that the resonant excitation of LRSP modes provided an amplified intensity of the magnetic field, which could be directly translated to an enhanced strength of fluorescent signals when the target was captured on the surface. With this improvement, the LRSP-FS was shown to have a LOD less than 10 CFU/mL with detection time of 40 min [52]. Although this technique is both rapid and sensitive for food safety detection, it requires an advanced surface plasmon device.

With the discovery of fluorophores, detection methods using fluorescence to label cells or their components allowed for visualization of images with greater contrast, compared to using a brightfield microscope [53]. Typically, there are several ways to specifically mark the proteins or

other structures of target cells, including fluorescent dyes, immunolabeling and fluorescent fusion proteins. For instance, a technique was developed using a fluorescent bacteriophage assay (FBA) approach with flow cytometry to detect *E. coli* O157:H7 cells in raw meat and raw milk. To prepare the bacterial beef samples, they added bacterial solution with required dilution to beef samples, then followed by adding them to Brain Heart Infusion (BHI) broth and incubated with shaking at 37°C for 6 h. To prepare the bacterial milk samples, they spiked raw milk with bacterial solution of the required dilution, then added the milk clearing solution, which was followed by centrifuged at 16000×g for 5 min. As a result, the bacterial pellet was resuspended in BHI broth and incubated with shaking at 37 °C for 10 h. The next detection process can be divided into two main steps. Immunomagnetic separation was first done to separate the target cells from the enrichment broth mixed with the immunomagnetic beads, and then a specific fluorescently stained bacteriophage was used to resuspend the separated magnetic beads for labelling the target cell. As a result of the detection with flow cytometry, the LOD of this FBA method was reported to be 2.2 CFU/g of contaminated raw meat after a 6 h enrichment step, and 10-10^2 CFU/mL of contaminated raw milk after a 10 h enrichment [54]. Recently, a newly developed method used the fluorescently labeled plant lectins as receptors to specifically recognize *E. coli* O157:H7 cells. The solution of FITC-labeled lectin was added to cell suspension and incubated for 20 min, followed by the analysis by flow cytometry. This method showed that the pathogens could be detected at a concentration of 10^6 cells/mL within 5 min [55]. This is a rapid assessment for preliminarily detection of contaminated food at a large scale.

Integrated systems are growing in the detection with respect to *E. coli* O157:H7 since it can shorten analysis time and increase detection efficiency. Recent research reported a development of a label-free amperometric biosensor for *E. coli* O157:H7 using a nano NiO film. This process involved an antibody-antigen reaction, where the antibody was bound to the surface of NiO thin film. Then, the accelerated charge transferred through NiO which was an external charge for the antibody. Charge transferred when the antigen bound to the antibody, which went through the NiO thin film, and this change of charge can be detected and was proportional to the amount of bacteria bound. This electrochemical sensor showed a wide linear range of 10 to 10^7 cells/mL and a low LOD of 1 cell/mL along with high specificity against other bacteria [56].

To conclude, an ideal detection method needs to satisfy primary requirements, including high specificity, high sensitivity, short detection time, simple operating procedure and cost effectiveness. For example, culturing takes a very long time to give the results. While nucleic acid based techniques, immunology based techniques and biosensors offer shorter waiting times, but these methods require the use of expensive reagents and sophisticated equipment [57]. Thus, the application of microfluidic systems, also known as micro total analysis systems (μTAS) have been used to integrate multiple operations and parallel identifications on a single miniaturized device with high throughput analysis [58]. Recently, increasing efforts have been put on the development of microfluidic systems for the detection of foodborne pathogens [10, 59-61]. In this study, the fabrication and development of a more effective microfluidic detection platform will be investigated.

2.2 Modification of PDMS microchannel for microfluidic detection

2.2.1 Polydimethylsiloxane (PDMS)

Polydimethylsiloxane (PDMS) is a silicon-based organic polymer and has been the most commonly used polymeric material for fabricating microfluidic devices. PDMS is a transparent, low-cost, biocompatible and soft elastomer. It is a viscous liquid form at room temperature and can be hardened after it is cured *via* crosslinking. It can be easily bonded with glass to package the microfluidic device. In addition, the whole fabrication process does not need a clean room [62].

2.2.2 Fabrication of PDMS microfluidic channel

To manufacture a PDMS microfluidic chip, soft lithography is the most commonly used method. It requires a mold to provide the hollow space of the microchannel, where the liquid sample will flow. Usually, the mold is made by photolithography. The process begins from using CAD software to create a design with a high-resolution commercial image setter, which may then be printed on a transparent plate. This is used as a photomask to produce a positive relief of photoresist on the silicon wafer. This modified silicon wafer is called a “master” to provide the hollow space for casting the PDMS microchannel. In order to produce the master, a SU-8 negative photoresist is a widely used epoxy-based photoresist. The negative photoresist means that the area treated by UV light will generate crosslink, while the untreated area is still soluble and can be washed off from the substrate. To manufacture the SU-8 master for the microfluidic channel, the

SU-8 liquid is poured onto the silicon wafer and spun with a selective speed to make an even surface with a desired thickness which will affect the depth of the microchannel. Then, the photomask is placed above the SU-8 surface to let UV light treat the surface, and subsequently the SU-8 surface is cured to solidify. After curing for a certain time period, a SU-8 developer is used to wash the SU-8 photoresist untreated by UV, and the treated parts will be left on the wafer to be the master of PDMS microchannel. A PDMS stamp is made by pouring a certain volume of liquid mixture of PDMS and crosslinker onto the master and cured into the solid phase, then the microchannel will be imprinted after removing it from the master. The resulting PDMS microchannel can be sealed with various substrates by using different chemical binding methods [63-65]. Oxygen plasma is generally used to seal the PDMS and glass, which introduces silanol groups (Si-OH) to the surface of PDMS and glass. The silanol group may then condense with the silanol group of another surface, generating a tight and irreversible Si-O-Si bond, especially after baking under a specific pressure [66]. Meanwhile, the inner surface of microchannel becomes hydrophilic, which may be verified by measuring the water contact angle. In addition, carbon dioxide, nitrogen and other inert gases also can be used to introduce the functional groups to the surface of microchannel [67]. The inner surface of the microchannel can be further modified by introducing the biochemical molecules to realize the detection, biochemical reaction and signal conversion [68-70].

2.2.3 Amination of PDMS surface

With respect to the modification methods, silanization is the most common way to introduce amine functional groups onto PDMS and glass surfaces. During this aminated process, the amino groups are introduced on PDMS surface. The amino-terminated PDMS surface is more stable than hydroxy-terminated surface because the modification of the former has been shown to impede the hydrophobic recovery of PDMS surface [71]. (3-Aminopropyl)trimethoxysilane (APTMS) and (3-aminopropyl)triethoxysilane (APTES) are commonly used silane reagents to introduce amino groups [72, 73]. Generally, after the treatment of oxygen plasma, the silane agent such as APTES can react with the hydroxyl group of PDMS surface to impart amino group with high stability.

2.2.4 Grafting of PAMAM dendrimers on the microfluidic channel

Polyamidoamine (PAMAM) is a class of dendrimer which is made of repetitively branched subunits of amide and amine functionally. It was first synthesized in 1984 and is also known as a "starburst polymer". This dendrimer is sphere-like, symmetrical, highly branching and has dense terminal functionality. Especially, PAMAM dendrimers with reactive end groups are monodisperse, and their molecular weights and numbers of branches can be controlled during the manufacturing process. The most commonly used approach for dendrimer synthesis is called the divergent method, in which the growth of dendrons originate from the core site [74]. The process of synthesis is through polymerization, and PAMAM dendrimers grow generation by generation and finally become highly branched tree-like structures as shown in Figure 1. To date, the maximum

generation of PAMAM dendrimers is tenth generation with 4096 functional end groups [75]. Since all the terminal groups can be modified, PAMAM dendrimers have versatile functions and can enhance the functionality of the microchannel after they are grafted on the surface of microchannel. For example, PAMAM dendrimers have been discovered to be a good choice in the field of drug delivery system [76]. Cheng *et al*. found PAMAM dendrimers were able to facilitate transdermal delivery of a nonsteroidal anti-inflammatory drugs (NSAID). The results showed that PAMAM dendrimers can effectively facilitate skin penetration of NSAID and have the potential ability to develop a new transdermal formulation [77]. In our previous study, PAMAM dendrimers were grafted on the inner surface of microchannel to conjugate with capturing structures. There are two principal functions of this application. One is to reduce non-specific adsorption of non-target particles, and another is to provide multiple binding sites for the capturing structures [24].

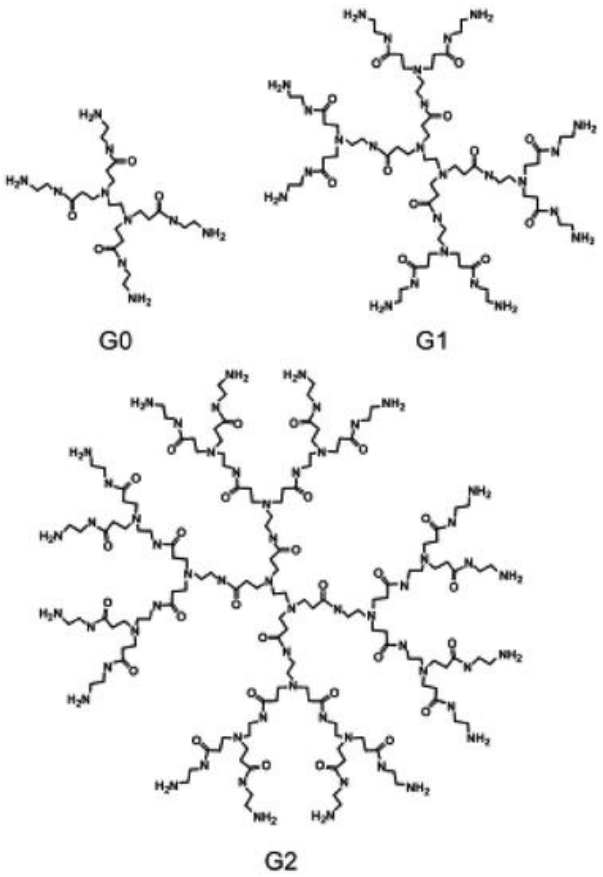

Figure 1. Structures of PAMAM dendrimers of several generations (*i.e.* G0, G1 and G2). Reprinted from Ref. [23], Copyright (2006), with permission from Royal Society of Chemistry.

2.3 Capturing structures for target cell recognition

2.3.1 Antibodies and antibody-based microfluidic detection

In terms of molecular recognition, antibodies have been widely used for diagnostic assays for more than three decades [78]. Antigen-antibody recognition system relies on the specific affinities of protein-protein, protein-carbohydrate or protein-DNA interactions. For instance, a microfluidic based biosensor was designed to detect and quantify the variation of magnetic field caused by the

presence of the magnetic beads bound to the antigens previously immobilized on the sensor surface by an antibody-antigen reaction [79]. A development for pathogen detection was a direct-charge transfer (DCT) biosensor. This device was fabricated using antibodies as the recognizing element and using a polyaniline nanowire as the signal transducer. This detection method was based on capillary flow action which allowed the liquid sample to flow from one membrane to another. The antigen-antibody reaction resulted in a direct electron charge flow, which generates a resistance signal. The whole detection time was completed in 6 min without any reagents, and the result of sensitivity was reported to be 10 to 100 CFU/mL [80]. Delehanty *et al*. reported an antibody microarray biosensor for the rapid detection for protein and bacteria under dynamic conditions. The biotinylated antibodies were printed and immobilized on the surface of a glass slide coated with avidins. Next, the antibody-based microarray system was used to detect microbial toxins with continuous fluid flow. The results of detection showed this device could simultaneously detect the cholera toxin and staphylococcal enterotoxin B in 15 min with LOD of 8 and 4 ng/mL respectively, *via* fluorescent-labeled antibodies and scanning confocal microscopy [81].

However, there are some limitations associated with antibodies. Firstly, since antibodies are generated *in vivo*, it is hard to obtain the antibodies against the molecule that is less immunogenic or intensively toxic. Secondly, the production of hybridomas is limited to rat, which restricts the usage of antibodies in therapeutic application. For instance, the heterophilic antibodies can link the capturing antibody with the secondary antibody without the target analyte, resulting in false-positive results [82]. Thirdly, the process of identifying and producing the monoclonal antibodies

are complex and even expensive for some rare antibodies [83]. Fourthly, antibodies are sensitive to the environmental temperature, and irreversible denaturation may take place [84]. Finally, the production of antibodies is affected by variations that may occur *in vivo,* which could cause the inconsistency of the function of antibodies from different batches [78].

2.3.2 Aptamers and aptamer-based microfluidic detection

In recent years, the development of the systematic evolution of ligands by exponential enrichment (SELEX) process has provided the potential for nucleic acid sequences to recognize the various analytes with high affinity and specificity. Such nucleic acid sequences are called "aptamers", which occur as the rival of antibodies in the diagnostic and therapeutic field. Aptamers were first introduced in 1990. They are synthesized single-stranded nucleic acid sequences which can specifically bind to a wide range of target molecules, such as ions, chemical compounds, DNA or RNA, proteins, and even whole cells.

In general, aptamers are screened *in vitro* by the SELEX technique. SELEX can be used to develop aptamers against various targets. As shown in Figure 2, the SELEX process starts with a library of random sequences. Each sequence in the library is a linear and unique oligomer. The complexity of a library is based on the number of random sequences. During the screening process, the random sequence library is incubated with the target molecule in the selective buffer at certain condition. As a result, there is a small portion of sequences in the library that can bind to the target, and these sequences are separated from the library by washing off the sequences which do not bind

to the target. The sequences bound to the target can be isolated and enriched for the next round of selection. The efficiency of the enrichment for high-affinity aptamers is under control of the requirement of selection of every round. The amount of selection rounds depends on the characteristics of the target and the stringency of each round. Generally, a typical SELEX process lasts 8-15 rounds, with one round taking 2 days. When the affinity is saturated after the selections round by round, the library of selective sequences is amplified and sequenced to obtain the information of each "winner" sequence. After the selection, the selected aptamers are usually 70-80 nucleotides in full-length and a part of nucleotide sequence will be eliminated to enhance the binding affinity of the aptamers with the target. Therefore, it is important to find a minimal target-binding domain in the selected aptamer. Finally, a selected aptamer is available for diagnostic assays after 2-3 months of the SELEX experiment. Jenison *et al.* developed an automated platform which can process multiple SELEX experiments in parallel on microtiter plates, thus significantly improving the efficiency of aptamer selection [85, 86].

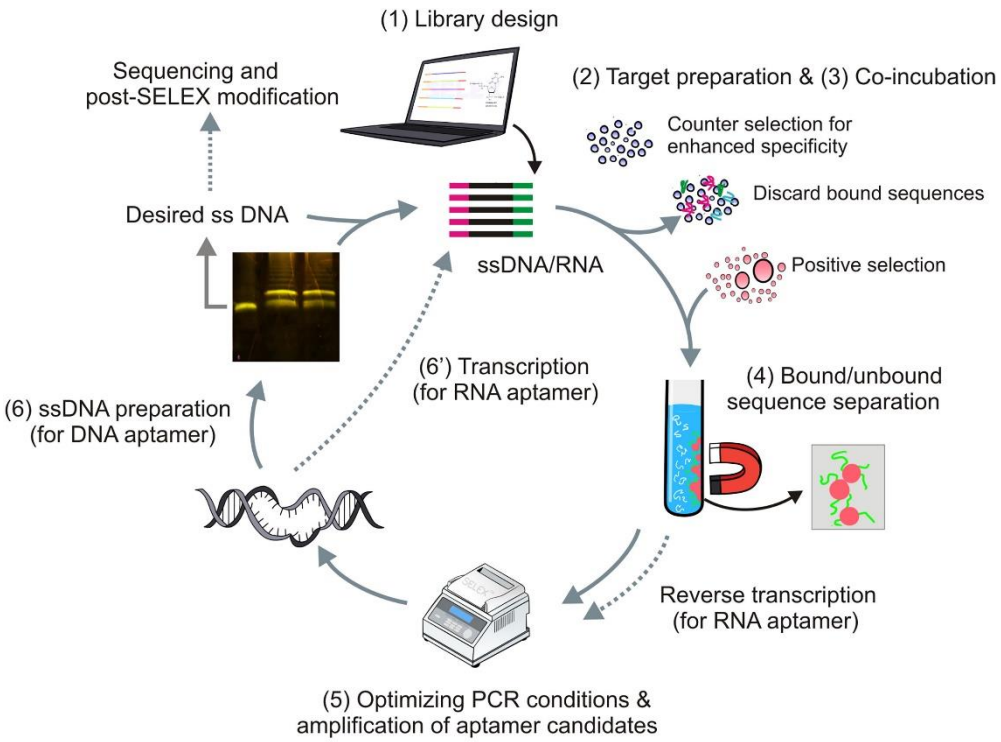

Figure 2. Illustration of the essential operations of a typical SELEX protocol, such as library design, target preparation, counter selection, co-incubation, selective sequence separation, aptamers amplification and post-SELEX modification. Reprinted from Ref. [87], Copyright (2019), with permission from Elsevier Science and Technology Journals.

Aptamers represent a potential alternative to antibodies as the capturing mechanism due to the challenges associated with antibody production. The use of aptamers has many advantages over conventional antibodies. For instance, aptamers typically exhibit higher stability, weak immunogenicity, greater consistency between batches, longer shelf life, and various possibilities for introducing chemical modifications to improve the affinity to their targets [88]. In the development of microfluidic detection, aptamers have been proven to be more sensitive and

specific than antibodies [89]. Unfortunately, there are also some problems that may limit the application of aptamers. For example, nucleic acid aptamers are susceptible to nuclease degradation which would seriously affect the structure and function of aptamers. Aptamers are also cleared rapidly from the body when used in whole organism through renal filtration [90, 91]. A recent review discussed several post-SELEX chemical modifications for improving the practical application of nucleic acid aptamers and several chemical modification strategies have been proposed, as shown in Figure 3 [92]. Research has revealed that the introduction of 3'-inverted dT modification and 3'-biotin could enhance the resistance of aptamers to 3'-exonucleases [93-95]. Modifications on the sugar ring of the nucleotide, such as 2'-O-methyl (2'-OMe) modification, was also reported to increase the ability of aptamers to resist nucleases and melting temperature [96]. In addition, it has been reported that modifying the 5'end with cholesterol, diallyl lipids and polyethylene glycol (PEG) could help to resist renal clearance [97-100]. Secondly, the binding affinity of aptamers may not be sufficient as therapeutic agents and need to be enhanced by post-SELEX modification. For example, a RNA aptamer approved by the FDA for treating a macular degeneration, was modified with different moieties to tightly bind with a human vascular endothelial growth factor (VEGF) [101]. Recent research has also shown that modification of the nucleotide sequence can be used to improve the binding affinity of aptamers [102].

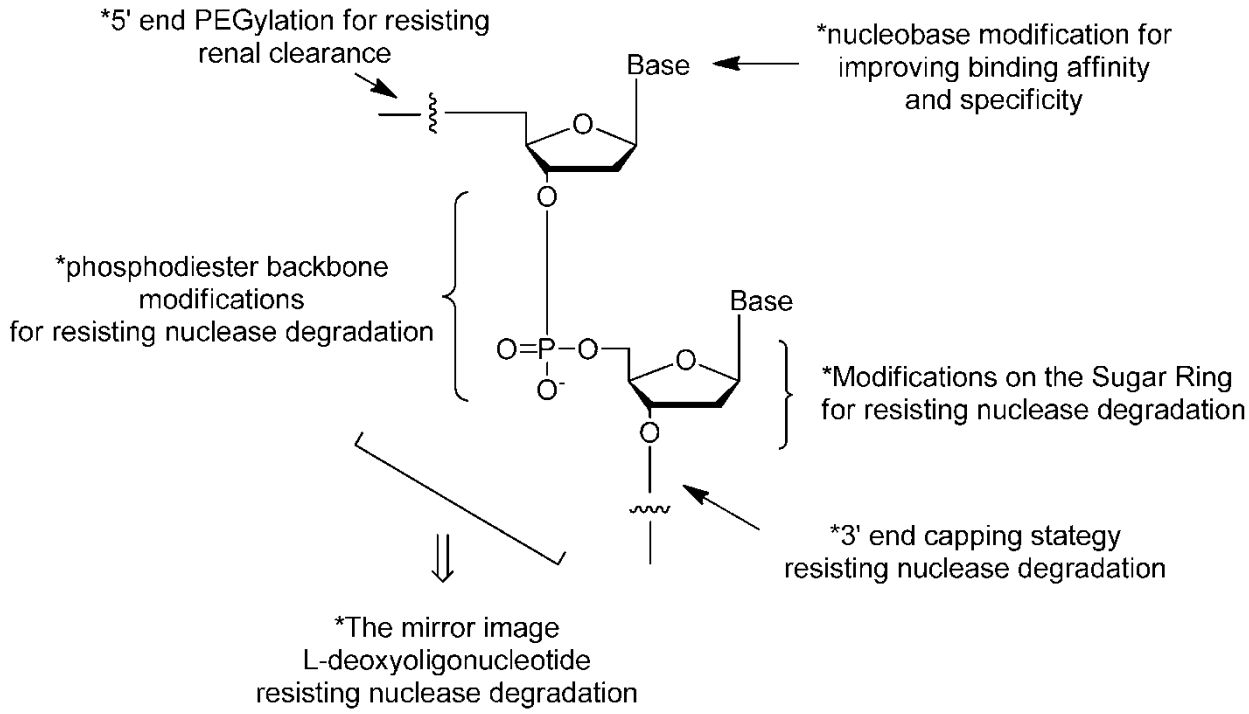

Figure 3. Schematic illustration of the common methods used to modify nucleic acid aptamers and their goals. The common approaches in the chemical modification of aptamers include nucleobase modification, modification on the sugar ring, 3' end capping with inverted thymidine, 5' end capping with PEGylation, phosphodiester backbone modifications and modification on the terminals of nucleic acids. Reprinted from Ref. [92], Copyright (2017), with permission from MDPI.

Recently, aptamer-based microfluidic detections have received a significant amount of attention in research. For instance, anti-thrombin aptamers have been used in a single-wall carbon nanotube (SWNT) biosensor to detect the serine protease thrombin. Aptamers were immobilized on the walls of SWNT with a field effect transistor. As aptamers were bound to SWNT, a right ward shift of the threshold gate voltages was generated due to the negative charge of the aptamers.

The results showed that the LOD of this device was 10 nM [103]. Because aptamers can be easily labeled with fluorophores, they have been applied to microchip electrophoresis as the probes. For instance, fluorescently labeled aptamers have been used to detect the trace amount of thrombin on using microchip electrophoresis [104]. Furthermore, an aptamer-based microfluidic device has been used to detect multiple cancer cells. More specifically, four wells were used as inlets and outlets of the microchannel and separated the microchannel into three regions. The three different regions were immobilized with different aptamers to recognize CEM, Ramos and Toledo cells respectively. This aptamer-based device included the cell pre-enrichment, target recognition and signal transduction, and was able to detect multiple cells at same time, which could be a useful tool in the field of cancer diagnostics [105].

2.4 Application of rolling circle amplification (RCA) for cell recognition

2.4.1 Introduction of RCA

Rolling circle amplification (RCA) is an isothermal DNA amplification where a short primer is amplified to generate a long single stranded DNA product using a circular DNA template and a polymerase. The resulting RCA product is a long concatemer which contains tens to hundreds of tandem repeating structures [106]. There are several essential factors in the RCA reaction: the DNA polymerase enzyme (*e.g.* phi29 DNA polymerase); a buffer solution compatible with the enzyme, the primer, the DNA template also called the padlock probe, and deoxynucleotide triphosphates (dNTPs). To carry out the RCA reaction, the linear DNA template and the primer are

ligated by DNA ligase (*e.g.* T4 DNA ligase) to form a circular DNA template. Subsequently, the DNA polymerase is added to the reaction mixture to initiates DNA elongation by adding the dNTPs to the 5' end of the primer, using the circular DNA template as the template. To characterize the RCA product, quantitative real-time RCA reactions and gel electrophoresis are widely used to evaluate the RCA products. A schematic of the RCA workflow and mechanism is illustrated in Figure 4, which shows the synthesis steps of circular template and the design of RCA reactions. As can be seen in Figure 4 (A), the synthesis of the circular template requires the hybridization of two linear sequences. This circular template can be used in various ways, with the typical RCA reaction being shown in Figure 4 (B) and 4 (C) depending on the specific polymerase is used. More complex methods that have been demonstrated are shown as well, such as a multi-primed template to generate multiple copies of the product in tandem as shown in Figure 4 (D). Since the RCA process can generate many DNA products from very few initial materials, and given that it is an isothermal process, RCA may be used in a diverse range of applications. For example, RCA has been applied in detection and diagnostic assays, in nanotechnology, and the material sciences [107].

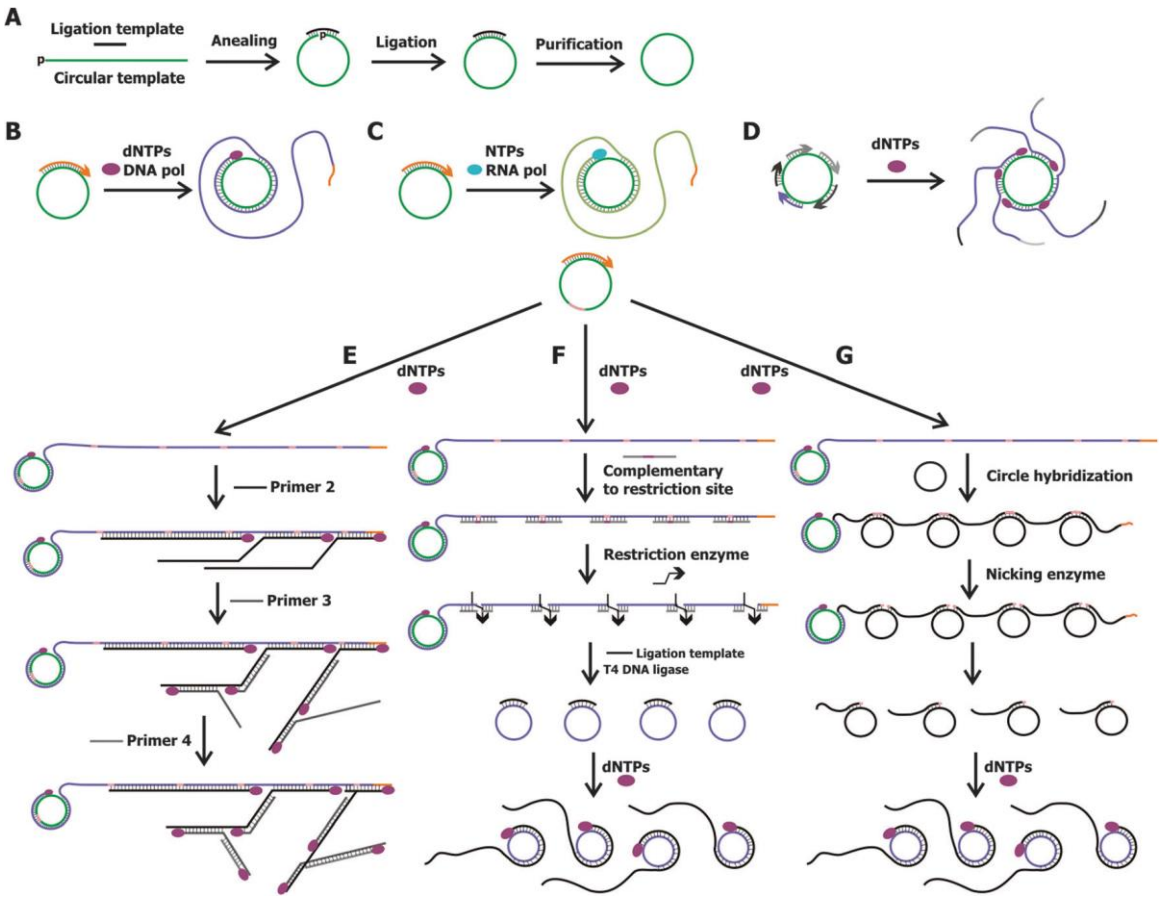

Figure 4. Schematic diagram of the basic principles of RCA. (A) Ligation process (B) Generate long and repeated ssDNA product *via* circular template (C) Generate long and repeated ssRNA product *via* circular template (D) Multi-primer hybridize with the circular template to generate ssDNA product (E) hyper-branched RCA (F) RCA generating multiple circular templates for next RCA (G) RCA generating primers for next RCA. Reprinted from Ref. [106], Copyright (2014), with permission from Royal Society of Chemistry.

2.4.2 Application of RCA process in detections

2.4.2.1 Detection of small molecules and proteins

The detection of small molecules and proteins uses circular templates to produce multiple binding sites for targets like antigens and proteins. Yang *et al*. designed an aptamer-based biosensor with RCA process, which was used to amplify the fluorescent detection signals. This RCA process was triggered by the capturing aptamer transformed to be circularized and can be ligated upon the interaction with the target platelet-derived growth factor (PDGF). The LOD was as low as 0.4 nM under real-time analysis [108]. Ou *et al.* proposed a novel sandwich liposome-RCA immunoassay to detect trace protein. The overall design is shown in Figure 5. This technology was based on DNA-encapsulating liposomes and liposome-RCA immunoassay. The liposomes were modified with antibodies for detection and encapsulate DNA primer probes. Due to the presence of the target, the modified liposome released the DNA primer probes which can initiate the RCA reaction, and the RCA product can be specifically detected through a fluorescence assay [107]. They also applied this technology to detect prostate specific antigen (PSA), a highly selective biomarker associated with prostate cancer. The results showed that this technique had a dynamic response to PSA over the concentration range of 6 orders of magnitude, from 0.1 fg/mL to 0.1 ng/mL, with a detection limit as low as 0.08 fg/mL and a high dose-response sensitivity. The DNA-encapsulated liposomes

based immunoassay showed very high sensitivity as a result of the introduced DNA probes which initiated large-scale DNA amplification [109].

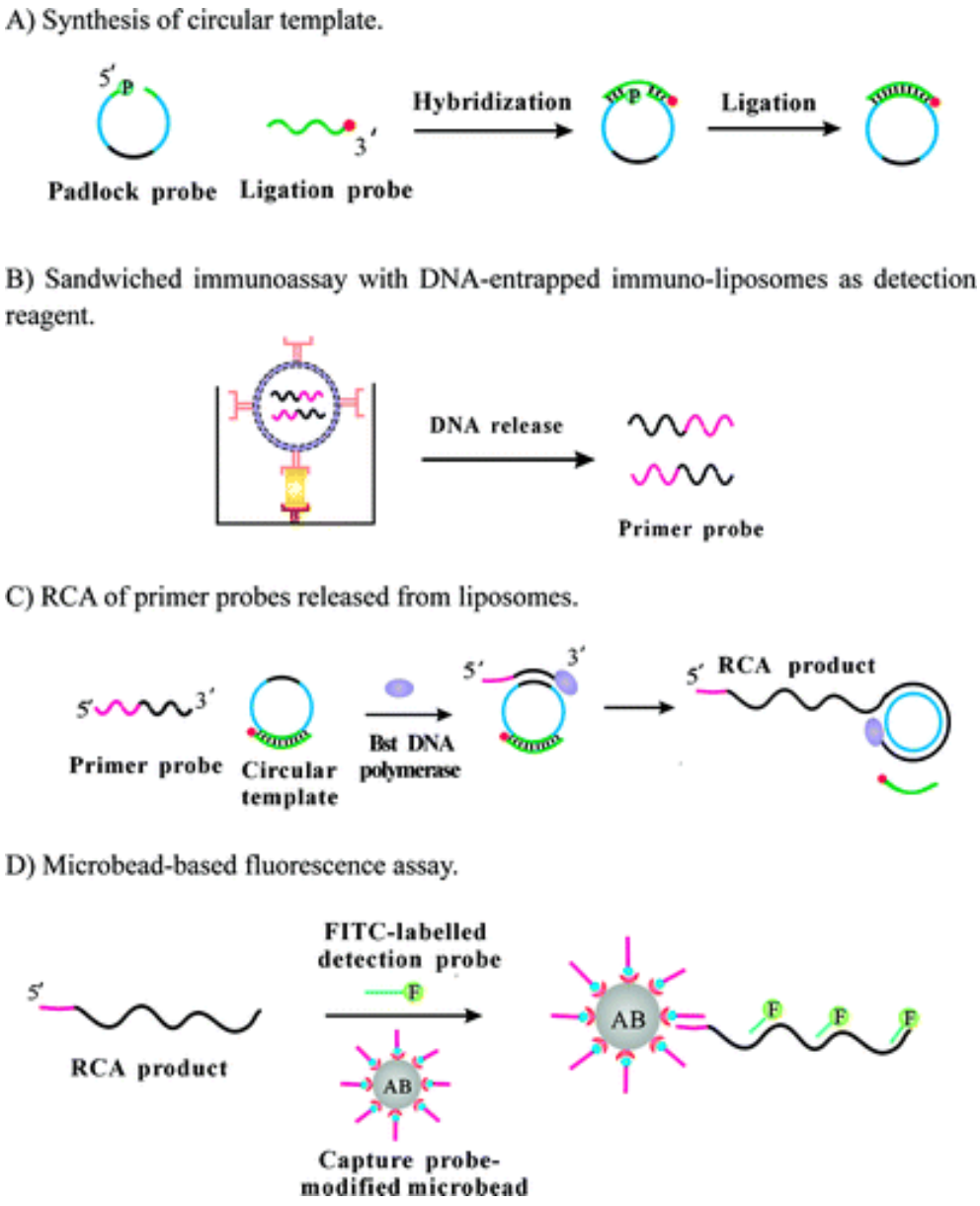

Figure 5. Schematic illustration of liposome-RCA immunoassay. (A) The synthesis of padlock probe; (B) The mechanism of PSA mediating the sandwiched immunoassay. The red sequences are primer probes of

biobarcode sequence, and the black sequences are universal primer sequence; (C) Primer probes start RCA reaction to produce a long tandem repeating molecule; (D) RCA products are hybridized with complementary FITC-labeled probes, then captured by capture probe modified microbeads. Reprinted from [109] , Copyright (2009), with permission from American Chemical Society.

2.4.2.2 Detection of DNA or RNA

Because of the high sensitivity of RCA reactions, many researchers are interested in combining this technique with the detection of specific DNA or RNA sequences, with the capability of even detecting single nucleotide polymorphisms (SNP). These applications will bring new ideas to diagnostic medicine and treatment of diseases. There are many methods utilizing RCA for the detection of DNA and RNA, and in general, they may be divided into two categories. The first method utilizes the target as a primer to trigger the RCA reaction by hybridizing with a circular template. This is relatively simple and avoids the low-efficiency step of ligation. The second method uses the target sequence or part of target sequence as a template to trigger the RCA reaction, including a ligation step to ligates both the ends of the linear RCA template, followed by a hybridization step to hybridize a short primer and the circularized template to initiate the long and repeating RCA products. The whole process is very strict and can not be made if there exists any mismatch, allowing for high target specificity, and provides a novel method for detecting mutations of nucleic acid sequences. For example, Rekha *et al.* adopted the RCA reaction with whole genome amplification (also called “WG-RCA”) to analyze the cell-free DNA of patient for

cancer surveillance and treatment. Instead of using a large amount of blood, they used a novel paper-based concept to collect fingerstick blood from the patient. After WG-RCA process, they identified somatic mutations from venous and amplified capillary samples by targeted sequencing and compared the detected mutations by droplet-digital PCR, which showed 100% agreement of mutations after whole genome amplification, and made great progress for longitudinal surveillance of metastatic cancer [110]. Qi *et al.* utilized the ligation-RCA to detect SNPs, using thermostable ligation for allele discrimination and applied RCA to the signal amplification. Through the SYBR-Gold stain, the discrimination can be viewed under UV light. Also, by combining the RCA reaction with this assay, small amounts of DNA samples are needed, which greatly reduces the cost of the whole detection process [111]. Yao *et al.* developed a gold nanoparticle (AuNP)-based lateral flow strip with RCA to detect some miRNA biomarkers (miRNA let-7a and miRNA 21), as shown in Figure 6. Specifically, this test strip was built with sample pas, NC membrane and absorbent pad topped on the PVC backing card. Before the assembly, the sample pad was soaked in the PBS solution and dried for storage. The test line and control line on the NC membrane were conjugated with the specific ssDNAs, followed by treated with streptavidin respectively, then dried for further assembly. To execute the detection, the test strip was insert into the well containing the mixture of RCA samples and AuNps-Probes. The result can be analyzed after scanning the test strip. The principle of the detection was based on the sandwich probes for the target detection. When there existed the target sequence, the RCA products would bound to AuNps-probes and then captured by the detection probes on the test line. The unbounded AuNps-probes could hybridize with the

detection probes on the control line. However, in the absence of target sequence, the detection probes on the test line would capture nothing while the AuNps-probes would be immobilized on the control line. Concerning the sensitivity of detection and experimental cost, it was important to combine RCA with their design. Furthermore, the high affinity and specificity of the DNA template (also called “padlock probes”) and targets made the time of detection fast [112].

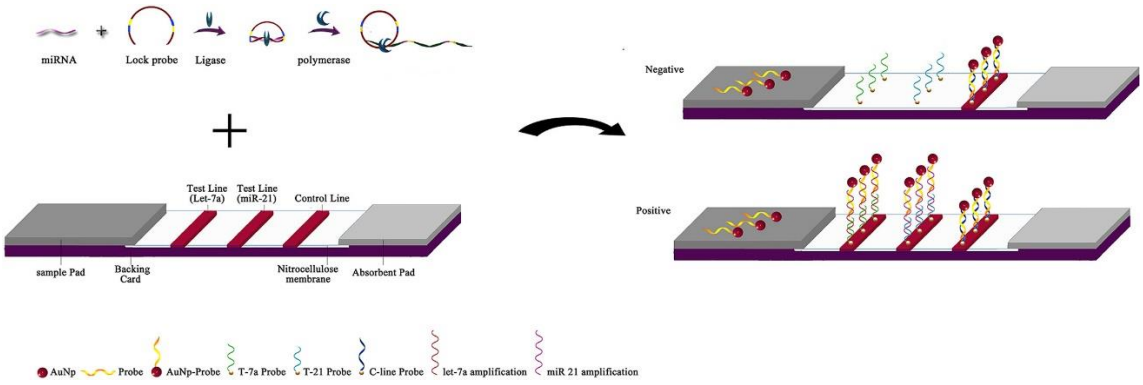

Figure 6. Schematic illustration of the AuNPs-based detection platform with RCA. Reprinted from Ref. [112], Copyright (2018), with permission from Elsevier Science and Technology Journals.

2.4.2.3 Detection of various pathogens

Many foodborne illnesses and deaths are related to the pathogenic bacteria. Further research on the rapid and sensitive diagnosis of these pathogens are important to public health and food safety. Traditional methods, such as cell culture and DNA extraction, in order to identify the foodborne pathogen are not effective enough in its current state. Therefore, further work must be done to develop methods which allow for fast and accurate detection of identifying various pathogens [11].

Enhancing the limit of detection is vitally important for early diagnosis. Due to the high efficiency of RCA reactions, it is typically coupled with biosensing methods for increasing the sensitivity of detections. Jiang *et al.* developed a dendrimer-aptamer-based microfluidic platform for *E. coli* O157:H7 detection and used RCA for the signal enhancement [113]. They adopted an aptamer which can specifically recognize and capture the target *E. coli* O157:H7 cells, immobilizing the cells on the inner surface of the PDMS microchannel *via* pre-conjugated PAMAM dendrimers. To further increase the detection signals and therefore the efficiency and sensitivity of the detection systems, RCA was performed on a template which would synthesize a product comprised of tandem repeats of a binding site of complementary fluorescence probes. As a result, the intensity of the detection signal was enhanced by up to 50 times and the LOD was reduced to 10^2 cells/mL with excellent specificity of detection. Moreover, research on developing an all-purpose detection system for concurrent identification of most pathogens are meaningful for improving the efficiency of detection [114]. In addition, a SPR biosensor achieved this goal for the detection of various pathogens, which utilized the refraction and reflection of light. During this process, the probes are immobilized on the surface of the sensor, and the target analytes are added to traverse these clusters continuously. Because of the sensitivity of this system, the whole detection system can be performed for real-time analysis [115].

2.4.2.4 Other novel detections

By conjugating the RCA products with functional nano molecules such as proteins, nucleic acids and nanoparticles [116], more and more applications have been developed and applied to different fields such as drug delivery, therapeutics and biosensing [106]. For example, the RCA product can be developed as a scaffold for the assembly of nanoparticles. A research group used the RCA products to form a 3D scaffold on AuNP for further assembly with a second set of nanospecies. The thiol-modified primers were conjugated with AuNPs then hybridize with a circular complementary template to initiate the RCA reaction for producing long DNA products. As a result, these resulting AuNPs-RCA product complexes can be design to form 3D DNA array [117].

2.4.3 RCA product as the biosynthesis aptamer for cell recognition

In the RCA product, the repeating structures can be generated into desired sequences given that the product strand is complementary to the sequence of the circular template. Based on this, scientists have developed RCA techniques to produce tandem repeating aptamers for the recognition of a specific target [14, 107, 118]. For instance, Zhang *et al*. developed a novel polyvalent therapeutic system which is composed of repeating aptamers synthesized by RCA and intercalated chemotherapy agents. The RCA synthesized multiple aptamers and doxorubicin constructed a poly-aptamer-drug system with 40-fold binding affinity with respect to the leukemia cells, compared to the monovalent aptamer system [15]. Zhao *et al.* incorporated RCA synthesized

aptamers bound to the enzyme tyrosine kinase which is overexpressed in many human cancer cells, into a microfluidic device and found that the RCA aptamers showed higher capturing efficiency than monovalent aptamers and antibodies [14].

To further improve sensitivity of the detection for *E. coli* O157:H7, this study also designed a RCA process to capture target bacterial cells (encoded as "cRCA"), which produced tandem repeating *E. coli* O157:H7 aptamers (encoded as cRCA aptamers), and proposed to replace the previous unit aptamers. The unit aptamers consist of a single and short sequence encoding the *E. coli* O157:H7 aptamer, while the cRCA aptamers consist of tandem repeating units of the same sequence of unit aptamer. The length of cRCA aptamer would reach several micrometers and can be used to specifically capture more target bacterial cells due to its branching structures. In other words, the cRCA aptamer modified microchannels should capture more target pathogenic cells than the modified microchannels using unit aptamers, given the equivalent concentration of inoculum.

2.4.4 Approaches to improve the efficiency of RCA reaction

Due to the inherent advantages, RCA-based systems have a wide range of prospects in the field of detection. In most applications, the time of detection relies on the time for executing the RCA process. Therefore, research on improving the efficiency of RCA reaction will significantly contribute to the development of rapid detection systems.

2.4.4.1 Modification of relative parameters

According to the inherent properties of the RCA process, there are several parameters related to the efficiency of the reaction, such as the length and the structure of padlock probes and primers, the efficiency of the enzymes and the reaction conditions [106]. Most research focused on modifying the sequence of the templates including both padlock probe and primer, since various structures of templates would greatly impact the result of the RCA reaction. Joffroy *et al*. discovered that a strong template length-dependent amplification efficiency bias of RCA, and concluded that an increased strain-promoted fraying probability could be the reason for increasing the rate of RCA reaction by comparing with a relaxed template [119]. Mao *et al*. found the DNA sequences with richness in adenosine (A) and cytidine (C) nucleotides tend to exhibit high efficiency during the RCA process. Also, these AC-rich sequences improved the sensitivity of the detection [120]. Miguel *et al.* modified the phi29 DNA polymerase by fusing DNA binding domains to the C-terminus of the DNA polymerase for increasing the efficiency of amplification. The chimeric polymerase was found to have enhanced DNA binding without hindering the replication rate [121].

One of the key steps in the RCA process is the ligation process. For this process, it is critical that the probe is fully hybridized to the target sequence in order to yield more circular templates. If there exists any mismatch around the junction part of the ligation templates, the padlock probes could not be circularized [106]. Cui *et al.* found the padlock probe without a terminal hairpin

readily formed polymeric linear by-products instead of a circular template. When there existed a hairpin near the 3’ or 5’ end, the linear padlock probe would be easily circularized with high selectivity [122]. Furthermore, pre-circularized template will be hybridized with the primer before the enzymatic reaction starts. Thus, the high-efficiency ligation will extremely improve the efficiency of the RCA process.

2.4.4.2 Introduction of external factors

Mikawa *et al*. found the mutant protein of single-stranded DNA binding protein (SSB) could improve the efficiency of RCA reactions. During this process, the reported protein also enhanced the specificity of phi29 DNA polymerase. In details, SSBs specifically bound to single-stranded DNA (ssDNA), and the presence of SSBs reduced the elongation time for phi29 DNA polymerase to generate RCA products, while also greatly reducing the formation of nonspecific RCA products [123]. Liu *et al*. reported an improved yield of RCA product by adding 15 μg/mL gold nanoparticles and shorten the time from 12 to 8 h as well. Moreover, they found the gold nanoparticles could bind specifically to RCA products [124].

Chapter 3. Experimental

3.1 General Approach

This study presents a strategy to improve the capturing performance of the microfluidic channel for *E. coli* O157:H7 detection. As shown in Figure 7, the inner surface of a microchannel is first activated with oxygen plasma, followed by surface amination *via* APTES treatment. Subsequently, PAMAM-COOH dendrimers are engrafted onto the aminated surface to provide multiple binding sites to conjugate c-primer/c-padlock probe ligation products (*i.e.* rolling circle template), in order to carry out the cRCA process from the channel surface. Under the catalysis of the phi29 polymerase, a long DNA molecule grows by adding the dNTPs to the 3' end of the c-primer using the c-padlock probe as a template, thus, forming many complementary sequences to the c-padlock probe. As a result, the cRCA reaction generates a very long, single-stranded DNA molecule that is comprised of tandem repeats of the capturing aptamer. In this experiment, the effectiveness of the cRCA approach in capturing *E. coli* O157:H7 cells is evaluated.

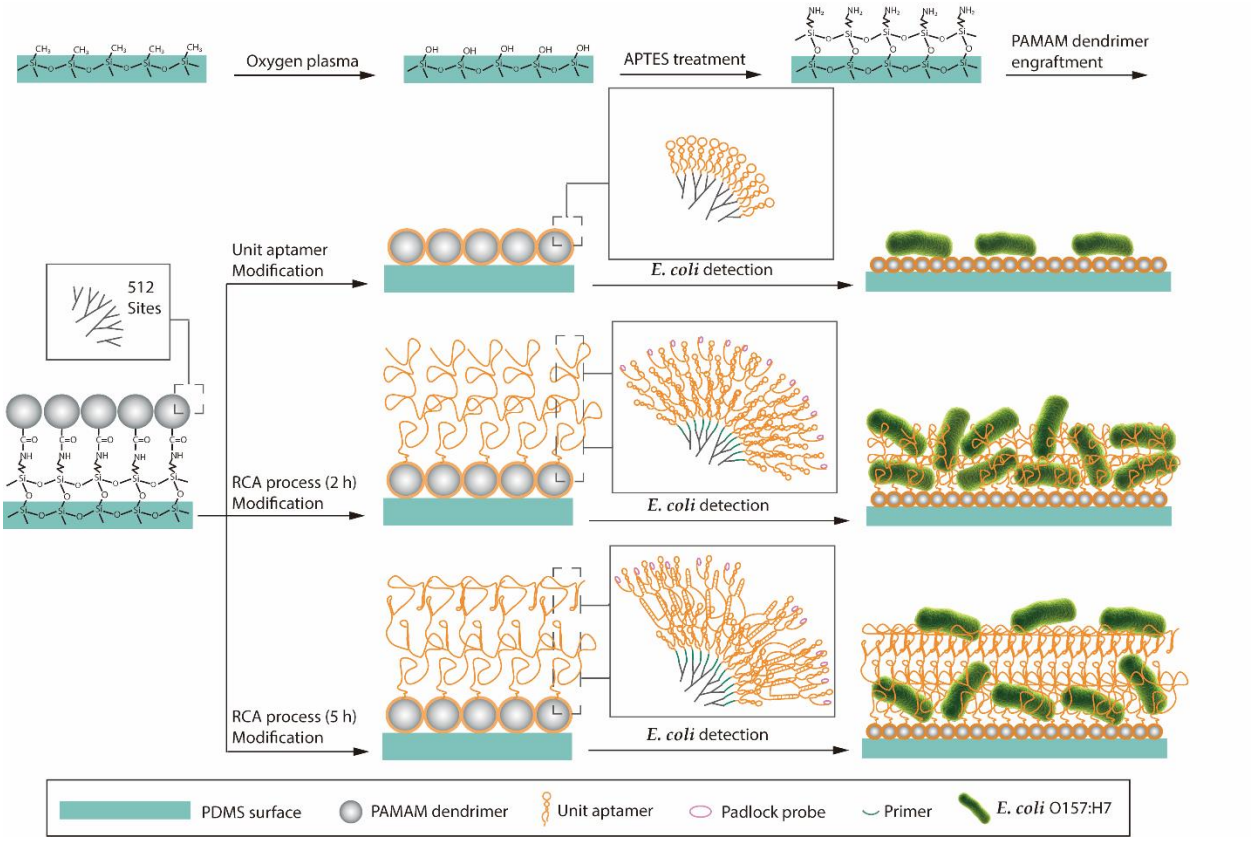

Figure 7. Schematic illustration to show the overall approach for the microfluidic channel surface modification, cRCA aptamer modification and *E. coli* O157:H7 detection. Note that above surface modifications were on all the inner surfaces of the microchannel.

3.2 Materials

Polydimethylsiloxane (PDMS) was produced using the Sylgard 184 silicon elastomer kit was purchased from Dow Corning (Midland, Michigan). Poly(amidoamine) dendrimer (generation 6.5, PAMAM-COOH), N-Hydroxysuccinimide (NHS) and (3-Aminopropyl)triethoxysilane (APTES) were obtained from Sigma-Aldrich (Oakville, ON). 1-(3-dimethylaminopropyl)-3-

ethylcarbodiimide (EDC) and 2-(N-morpholino)ethanesulfonic acid (MES) were purchased from Alfa Aesar (Ward Hill, MA). DNA oligonucleotides (sequences shown below under Table 2) and IDTE pH 8.0 solution were obtained from Integrated DNA Technologies (Coralville, IA). Phi29 DNA polymerase, T4 DNA ligase, deoxynucleotide triphosphate (dNTP) solution mix and SYBR Gold nucleic acid gel stain were purchased from Thermo Fisher Scientific (Burlington, ON). Heat-killed fluorescein isothiocyanate (FITC) labeled target *E. coli* O157:H7 cells and non-target *E. coli* ATCC25922 cells were generous gifts from the Canadian Food Inspection Agency (Ottawa, ON). All other chemicals were obtained from VWR International, LLC Canada unless indicated otherwise.

Table 2. The detail of DNA sequences used in this study.

Name	Sequence (5'—>3')	Ref.
Unit aptamer	NH_2-ATCG TCACA CCTGC TCTAT CAAAT GTGCA GATAT CAAGA CGATT TGTAC AAGAT GGTGT TGGCT CCCGT AT	[12, 125]
cRCA aptamer-primer (c-primer)	NH_2-TTTTT TTTTT GAAGG ACTTA GTTAC TGTCG AGCGA T	This work
cRCA aptamer-padlock probe (c-padlock probe)	AACTA AGTCC TTC*AT ACGGG AGCCA ACACC ATCTT GTACA AATCG TCTTG ATATC TGCAC ATTTG ATAGA GCAGG TGTGA CGGAT* ATCGC TCGAC AGT	This work
Fluorescent probe complementary to cRCA aptamer	Cy3-TTTTC TTGTA CAAAT CGTCT	This work
sRCA product-primer (s-primer)	NH_2-TTTTT TTTGT CCGTG CTAGA AGGAA ACAGT TAC	[126]
sRCA product-padlock probe (s-padlock probe)	TAGCA CGGAC ATATA TGATG GACCG CAGTA TGAGT ATCTC CTATC ACTAC TAAGT GGAAG AAATG TAACT GTTTC CTTC	[126]

Note: The italic portion in the sequence of c-padlock probe is complementary to the sequence of unit aptamer, in order to produce tandem repeating copies of unit aptamer. The cRCA aptamer is produced by using the conjugation product of c-padlock probe and c-primer as template (*i.e.* rolling circle template) and it contains repeating sequences that are complementary to the fluorescent probe. The underlined sequence in the c-padlock probe and fluorescence probe (complementary to cRCA aptamer) are same sequence.

3.3 Methods

3.3.1 Microchannel fabrication and PAMAM dendrimer engraftment

To fabricate the microchannel, a PDMS stamp was fabricated from a standard soft lithography process [127]. In general, a SU-8 master of the microchannel was prepared *via* a 19-μm-thick layer SU-8 2025 which was patterned by photolithography on top of a 4-inch silicon wafer. Sylgard 184 elastomer and the crosslinker were mixed thoroughly at a 10: 1 ratio (w/w) and poured on the top of the master, which was followed by degassed for 30 min and then cured at 85°C for 2 h, after which the PDMS stamp was removed from the SU-8 master. Next, two holes were pierced through the prepared microchannel as the inlet and the outlet, and was subsequently bonded with a glass slide after treatment with oxygen plasma using a plasma etcher (SP100, Anatech Ltd, Battle Creek, MI) at 100 m Torr, 118 W for 10 s. Finally, the sealed microchannel was kept at 100°C for 30 min to achieve irreversible bonding [128]. To conjugate PAMAM dendrimers onto the inner surface of the microchannel, a previously established silane coupling method was used with minor modifications [128, 129]. Briefly, 5 wt.% APTES was used to treat the microchannel for 20 s in order to aminate the inner surface by silanol condensation. This step was followed by sequential washes with absolute ethanol, 95% ethanol, 70% ethanol and water. Finally, the aminated microchannel surface was filled with 10 μM PAMAM-COOH, 1 mg/mL NHS and 1 mg/mL EDC in 0.1 M MES solution (pH 6.0) at room temperature for 2 h to immobilize PAMAM-COOH to the inner surfaces of the microfluidic channel.

3.3.2 *In situ* cRCA reaction on microchannel surfaces

The *in situ* cRCA reaction started with the preparation of the circular template. To prepare the circular template, 2 μL c-padlock probe (100 μM) and 2 μL c-primer -NH_2 capped (100 μM) were mixed in 84 μL nuclease-free water. The mixture was first heated to 95°C for denaturing, then followed by ice cooling for 1 min and hybridized at 37°C for 30 min incubation. Next, 12 μL of ligation buffer (including 10 U of T4 DNA ligase, 10X buffer) was added into the reaction mixture to react at room temperature overnight. Then the reaction mixture was heated at 65°C for 10 min to deactivate T4 DNA ligase in order to stop the ligation reaction. The final product of the reaction was circular template capped with -NH_2.

To synthesize the cRCA aptamer, the resulting -NH_2 capped circular template (0.2 μM) was first immobilized onto the PAMAM-COOH modified surface of the microchannel using an NHS and EDC chemistry. Briefly, the phi 29 polymerase would initiate the cRCA process by adding dNTPs to the 3' end of -NH_2 capped c-primer along with the circular template. To carry the cRCA reaction, a 100 μL reaction mixture containing 10X phi29 buffer, 0.4 mM dNTPs and 10 U phi29 polymerase was injected into the microchannel at a flow rate of 0.05 mL/h. The reaction was allowed to be carried out at 37°C for a pre-determined period of time (*i.e.* 0.5, 1, 2, 3 and 5 h). At the end of the reaction, the reaction mixture was heated to 65°C for 10 min to inactivate the phi29 polymerase to stop the reaction.

3.3.3 Characterization of the cRCA product

To investigate the cRCA reactions, a Bio-Rad CFX Connect Real-Time PCR Detection System (Canada) was used to monitor the reaction in real-time. In a typical cRCA reaction, the reaction mixture was composed of different concentrations of the circular template and c-primer (*i.e.* 0.05, 0.1 and 0.5 μM), phi29 reaction buffer, 0.1 U/μL of phi29 DNA polymerase, 125 μM of dNTPs, 0.2 μg/μL of BSA, and 1X SYBR Gold in a total volume of 20 μL nuclease-free solution. The reaction mixtures were prepared on ice to prevent a premature start of the cRCA reactions. The qPCR was set to run isothermally at 37°C for 5 hours, and during each run, the relative fluorescent signals were collected every minute under the SYBR setting. In parallel, samples without circular template was used in otherwise identical runs as negative controls.

To verify that the cRCA aptamer can be carried out *in situ* on PAMAM dendrimer modified PDMS surfaces, pristine PDMS surfaces were initially modified with PAMAM-COOH dendrimer, followed by a modification by an *in situ* cRCA reaction, as outlined in Section 3.3.2. Subsequently, complementary Cy3 probes were used to detect the cRCA reaction product under an Olympus fluorescence microscope (IX81, Richmond Hill, ON). The fluorescence intensity was documented using a high-resolution camera (QImaging, Surrey, BC) and analysed using NIH ImageJ software (National Institute of Mental Health, Bethesda, Maryland, USA). In measuring the fluorescence intensity, eight random and different spots were measured from each sample, and then their average value was taken as the average fluorescence intensity of the given sample; average values of three

parallel samples were used to calculate the surface fluorescence intensity of a sample of interest. All measurements were performed under identical exposure times. PAMAM-COOH dendrimer modified surfaces and unit aptamer modified surfaces were also used as controls.

3.3.4 Microchannel capturing performance for target E. coli O157:H7 cells

In order to evaluate the capturing performance of cRCA aptamer modified microchannels for *E. coli* O157:H7 cells, FITC labeled target cells were introduced into the capturing microfluidic channels for 1 h, and the captured cells were manually counted under the fluorescence microscope. For each microchannel, sixty continuous fluorescent images were also collected and then analyzed by NIH ImageJ software. To compare, the capturing performance of both PAMAM-COOH dendrimer modified microchannels and the unit aptamer modified microchannels were used as controls. The experiments were conducted in triplicate.

3.3.5 Capturing specificity

To investigate the capturing specificity of all the cRCA aptamer-based detection platform, target *E. coli* O157:H7 cells and non-target *E. coli* ATCC25922 cell were separately injected into different microchannels. Specifically, both cells were individually doped into iced tea at a concentration of 10^4 cells/mL, and injected into the microchannels at a volumetric flow rate of 0.5 mL/h. Finally, the captured cells were manually counted, using the method discussed in Section 3.3.4. All the experiments were conducted in triplicate.

3.3.6 Optimization for capturing performance of cRCA aptamer-based microchannel

To improve the detection efficiency, a functional cell-capture assay was conducted under controlled reaction time of cRCA process and dynamic flow conditions *via* orthogonal experiments. The boundary values of reaction time were 0.5 and 5 h, and flow rates were 0.01 and 1 mL/h. The capturing performance of the microchannel under each condition was measured as described in Section 3.3.4. A two-way ANOVA test ($\alpha = 0.05$) was used to evaluate the effect of reaction time of the cRCA process and flow rates on capturing performance of the microchannels. To compare, the capturing performance of both PAMAM-COOH dendrimer modified microchannels and unit aptamer modified microchannels were used as controls. The experiments were conducted in triplicate.

3.3.7 AFM characterization of cRCA products and structure prediction

Atomic force microscopy (AFM) characterization was used to study the cRCA reaction products. Specially, 5 μM of cRCA products solution was dropped on a mica surface (V-1 Grade, SPI Supplies Division of Structure Probe Inc., West Chester, PA) and was carefully washed with double-distilled water for 1 minute then air-dried. The resulting sample was imaged by a Multimode AFM with NanoScope V controller (Bruker Nano Surfaces Division, Santa Barbara, CA) in either Bruker's ScanAsyst or PeakForce QNM modes. The obtained images were analyzed using Gwyddion software (Brno, Czech Republic). For each sample, 500 cross-sections were

measured from 10-20 images. In addition, the length of cRCA products were measured by DNA trace software (Laboratory of Physics of Living Matter, EPFL, Switzerland).

The secondary structures of unit aptamer and cRCA products were simulated at their lowest free energy [130-132]. The 10, 20 and 40 copies of unit aptamer sequence were simulated using an RNA structure software (Mathews lab, Rochester, NY) to predict the most likely structures of the molecules of interest.

3.3.8 Water contact angle

To confirm the layer-by-layer surface modifications, a goniometer (AST Products Inc., Billerica, MA) was used to measure water contact angle of surfaces of interest (*i.e.* the pristine PDMS surface, oxygen plasma treated surface, APTES modified surface, PAMAM-immobilized surface, unit aptamer engrafted surface and cRCA products engrafted surface). For every measurement, 1 μL of double-distilled water was dropped on the surface of interest. After the needle tip was withdrawn from the droplet, the water contact angle could be measured by approaching the surface to the field of camera. Three random and different areas were measured on each surface. All the experiments were repeated in technical triplicate.

Chapter 4. Results and Discussion

4.1 Characterization of cRCA products

4.1.1 Real-time quantitative analysis of cRCA reaction

To confirm that the cRCA reactions can be successfully carried out, real-time quantitative analysis was used to characterize the cRCA products. Specifically, real-time quantitative analysis of the cRCA reaction was achieved utilizing SYBR Gold, a dye which intercalates into the single-stranded cRCA products during the rolling process. The resulting fluorescence-reaction time curves were dependent on the concentration of the initial templates (*i.e.* c-padlock probe and c-primer) as shown in Figure 8 (A), while the results of the control group without templates were not displayed since there was no obvious fluorescent signal generated. In these exhibited reactions, the fluorescent signals increased with cRCA reaction time. When the concentrations of the initial templates were 0.1 and 1 μM, the fluorescent signals increased rapidly at the beginning of the reactions, followed by increased at the slower rate, which could be caused by the gradual exhaustion of phi 29 polymerase. This suggested that the cRCA reaction only needs a short time period (less than 2 h) to produce a detectable signal for the cRCA reaction. The slope of the fluorescence-reaction time curve is steeper for the cRCA reactions with a higher concentration of the initial templates. The reaction rate can be measured from the slopes of these curves based on initial signal increment. For example, at first 60 min, the reaction rates were calculated *via* the linear fit of the fluorescence curves, as shown in Figure 8 (B). The reaction rate increased with

increasing concentrations of initial templates. Furthermore, it was verified that the cRCA reactions performed appropriately in the solution.

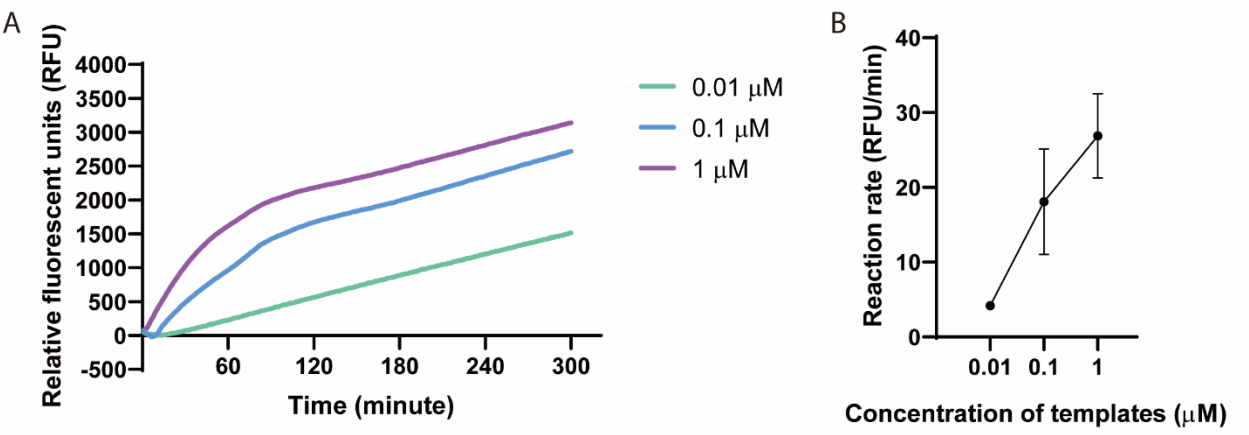

Figure 8. (A) Fluorescence-reaction time curves of cRCA reactions for quantitative detection of cRCA products with varied concentrations of initial templates and (B) reaction rate as a function of concentration of initial templates at the reaction time of 60 min.

4.1.2 Fluorescence test of cRCA aptamer modified PDMS surface

In order to confirm that the cRCA reaction can be indeed carried out on the PDMS surface and produce functional long single-stranded DNA products, circular templates that were capped with $-NH_2$ were introduced to the PDMS surface *via* PAMAM-COOH to start the cRCA reaction. Subsequently, complementary fluorescent probes were used to hybridize with the cRCA products, and the fluorescence intensity of the resulting surfaces was investigated. As shown in Figure 9 (A), it is evident that PDMS surfaces modified with cRCA products showed significantly enhanced

fluorescence intensity in comparison with the PDMS surface solely modified with the unit aptamer, which suggested that cRCA products contained multiple repeating structures of the unit aptamer. It is worthwhile to note that the fluorescence intensity initially increased with increasing cRCA reaction time as expected. However, the fluorescence intensity started to decrease when cRCA reaction time was carried out over 2 h. In addition, Figures 9 (B) to (E) show the representative fluorescence images for all the conditions of the PDMS surfaces mentioned in Figure 9 (A), with the exception of the PAMAM dendrimer modified surface. The results indicated that the structures of cRCA products on the surface changed unexpectedly when the cRCA products were elongated to a certain degree.

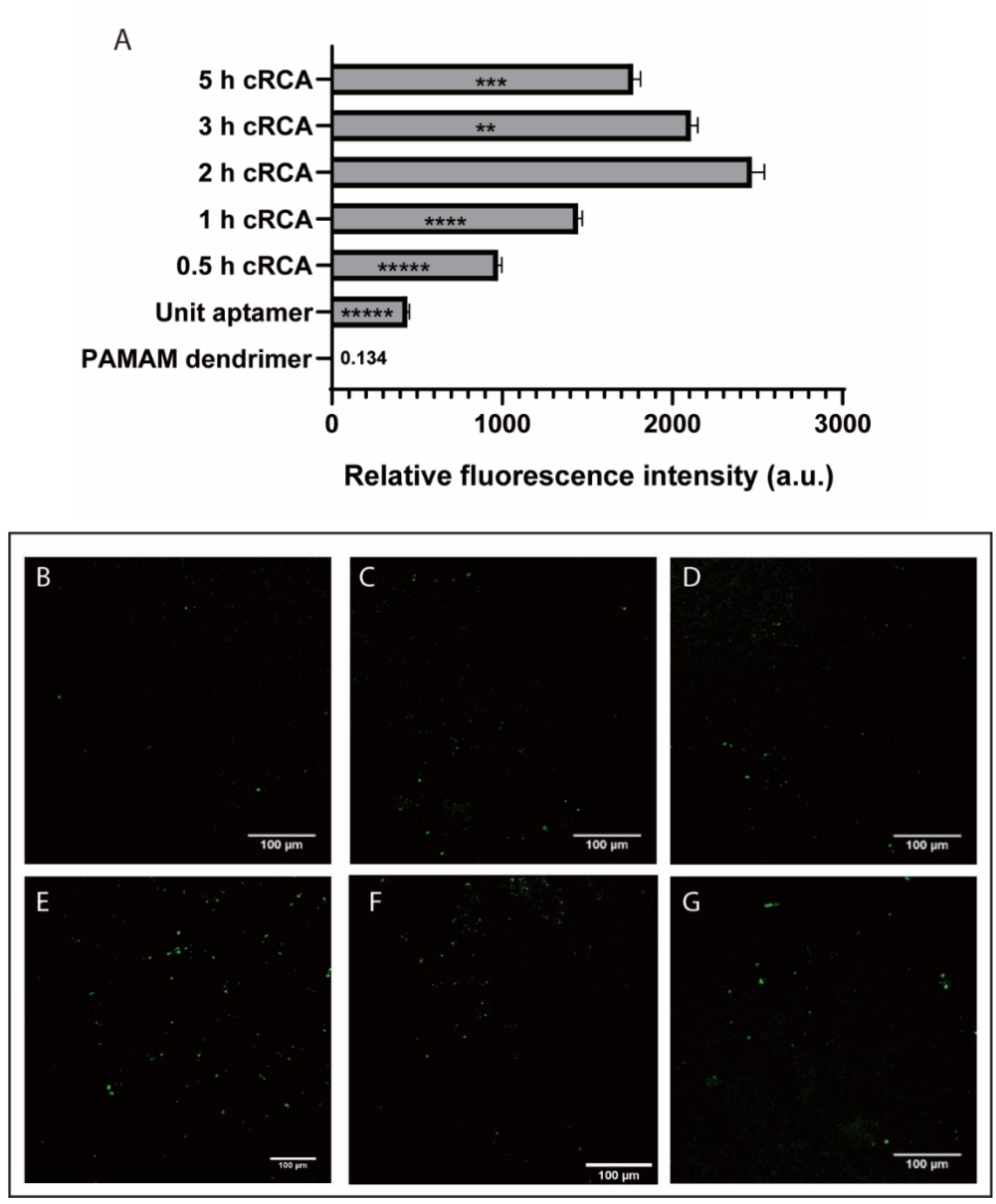

Figure 9. (A) Relative fluorescence intensity of PDMS surface modified with PAMAM dendrimer, unit aptamer and cRCA products; representative fluorescence images of (B) unit aptamer modified surface, (C) 0.5 h cRCA products modified surface, (D) 1 h cRCA products modified surface, (E) 2 h cRCA products modified surface, (F) 3 h cRCA products modified surface and (G) 5 h cRCA products modified surface. All the experiments were conducted in triplicate.

4.2 Capturing specificity

In order to test the specificity between cRCA aptamer and *E. coli* O157:H7 cells, the optimal cRCA aptamer (*i.e.* 2 h cRCA products) modified microchannel was used to detect the *E. coli* O157:H7 contaminated iced tea. Meanwhile, *E. coli* ATCC25922 cells are not targeted, and were used as a control for *E. coli* O157:H7 cells, while the non-specific sequence (*i.e.* sRCA products, which were produced by s-primer and s-padlock probe) was used as a control sequence for cRCA products. As expected, the cRCA product should consist of repeating capturing sequences which are specific to the O-antigen of lipopolysaccharides on the surface of *E. coli* O157:H7 [12]. The results showed the number of target cells captured by cRCA products was significantly larger than that of the other three conditions (Figure 10 (A)), which suggested the biosynthesised cRCA aptamer was specifically binding with *E. coli* O157:H7 cells. Also, the representative fluorescence images in Figure 10 (B) showed that a large amount of target cells were specifically captured by cRCA products, while only several non-target cells were observed in the identical modified microchannel. Moreover, sRCA products did not exhibit the obvious capturing ability for either target or non-target bacterial cells. This result is essential because it not only shows the feasibility of the cRCA aptamer-based microfluidic detection system, but also demonstrates the potential of developing a dual-RCA detection system. To summarize, the cRCA products will be used to

capture target cells while the sRCA products will be responsible for amplifying the detection signals to achieve better sensitivity.

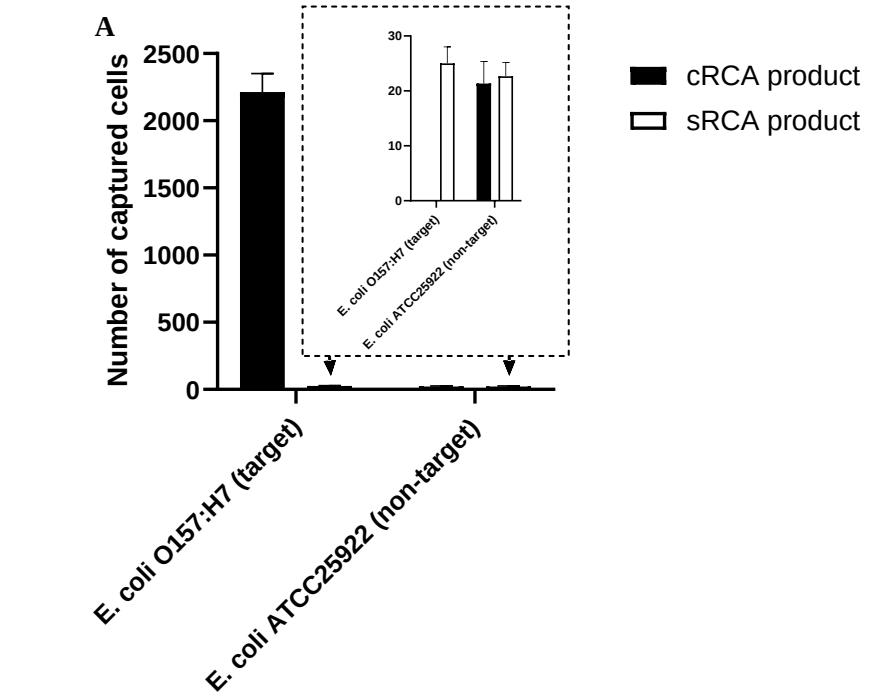

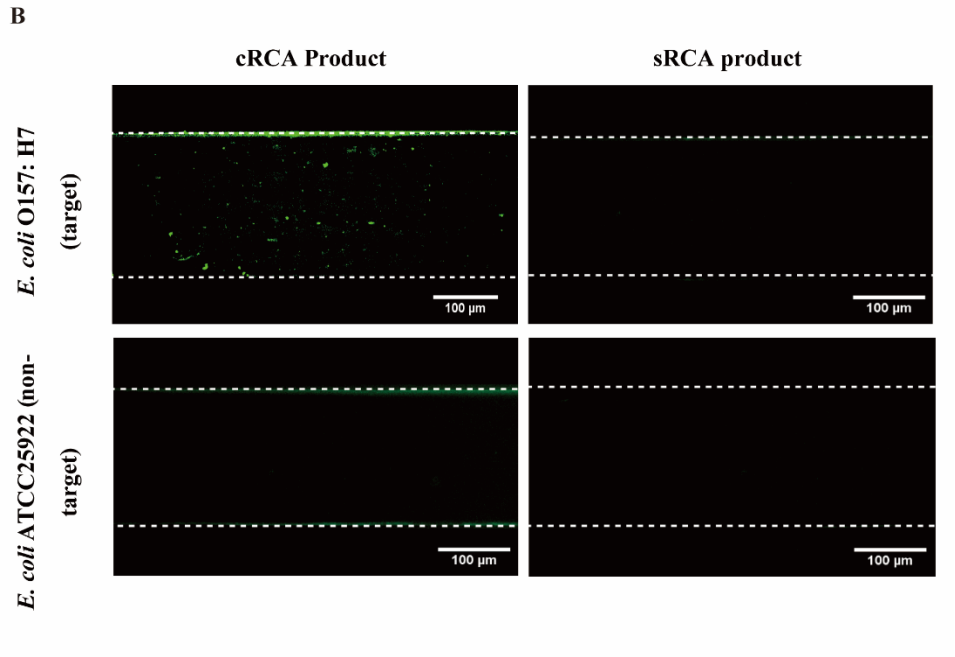

Figure 10. Specificity test of the optimal cRCA aptamer-based microchannel for detecting target *E. coli* O157:H7 cell in iced tea. Non-target *E. coli* ATCC25922 cells were used as a control for *E. coli* O157:H7 cell while the sRCA products were used as a control sequence. All the experiments were conducted in triplicate. (A) The number of target cells and non-target cells respectively captured by cRCA aptamer-based microchannels and sRCA products modified microchannels; (B) representative fluorescent images of FITC labeled target cells and non-target cells captured in cRCA aptamer-based microchannels and sRCA products modified microchannels.

4.3 Optimization for capturing performance of cRCA aptamer-based microdevice

In this study, cell capture assays of cRCA aptamers modified microchannels were conducted under controlled dynamic flow conditions to promote the detection efficiency. The capturing performance was investigated by injecting a PBS solution spiked with 10^4 cells/mL of *E. coli* O157:H7 for 1 h. The unit aptamer modified microchannel and generation 6.5 (G6.5) PAMAM dendrimer modified microchannel were used as the control system. Under controlled dynamic condition, the capturing performance of cRCA aptamer initially displayed an increasing trend within the first 2 h of reaction, but started to decrease thereafter. Moreover, the 2 h cRCA aptamers showed significantly stronger capturing performance, followed by the 3 h, 5 h, 1 h, 0.5 h cRCA products and unit aptamer, as shown in Figure 11 (A). In Figure 11 (A) and (B), the 2 h cRCA aptamer can capture more target cells than the 0.5 h and 1 h cRCA aptamers, since a longer reaction time would theoretically generate more repeating products [16, 106]. Unexpectedly, the 3 h and 5

h cRCA aptamers did not capture more cells than the 2 h cRCA aptamer under all the dynamic flow conditions. However, this result is consistent with the fluorescence test in Section 4.1.2, and it also suggests that the structures of cRCA products changed as a result of the additional reaction time, which resulted in the loss of capturing structures.

The variation of flow rates showed a certain effect on the capturing performance of both unit aptamers and cRCA aptamers modified microchannels, as illustrated in Figure 11 (B). In general, cRCA aptamers modified microchannels exhibited significantly better cell capturing performance than the unit aptamers at the flow rates ranging from 0.01 to 1 mL/h (corresponding shear stress from 0.166 dyn/cm^2 to 16.279 dyn/cm^2 on the wall). With increasing flow rates, the numbers of captured cells for the unit aptamer and all the cRCA aptamers initially increased then decreased. Notably, all the cRCA aptamers (0.5 - 5 h) achieved their best capturing performance at 0.5 mL/h, while the unit aptamer reached a plateau. Considering that the cRCA process will be used in the dual-RCA based detection system, the signal will be amplified based on the number of captured target cells [17, 126], and therefore, the optimal flow rate for this cRCA aptamer modified microchannel is 0.5 mL/h.

At given flow rates, capturing performance of all the modified microchannel were analyzed by a two-way ANOVA test ($\alpha = 0.05$), as seen in Table S1 of Appendix. When the flow rate was relatively low (*i.e.* 0.01 and 0.05 mL/h), there was no significant difference between the various aptamers modified microchannels. When the flow rate was increased to 0.1 mL/h, the difference

between unit aptamer and cRCA aptamers became noticeable, and the difference became even greater between 0.5 mL/h and 1 mL/h.

The data of capturing performance of all modified microchannels at controlled dynamic flow condition were also analyzed using a two-way ANOVA comparison test (as shown in Table S2 of Appendix). In general, the cRCA aptamer modified microchannels showed better capturing performance than that of the unit aptamer modified microchannels. In the case of the unit aptamer modified microchannels, the capturing performance increased as the flow rate increased until it achieved a maximum at the flow rate of 0.5 mL/h, and then started to decrease. In the case of cRCA aptamer modified microchannels, for the shorter cRCA reaction time (0.5 and 1 h), the capturing performance was affected by flow rates; longer reaction time (2 h, 3 h and 5 h) showed significant difference of capturing behavior at different flow rates. Moreover, the differences in the number of cells captured between each group became greater as the flow rate increased from 0.01 mL/h to 0.1 mL/h.

However, Figure 11 (C) revealed that the capturing efficiency of the cRCA aptamer decreased with the increase of flow rate, despite the fact that the total number of cells injected into these microchannels would correspondingly increase. This indicates that these modified microchannels had their limitations of capturing function [133]. Due to a relatively higher shear stress at 1 mL/h, the cRCA aptamer could not capture the target cells as much as at 0.5 mL/h [134], which resulted in a sharp decrease of capturing efficiency. Overall, it is worth mentioning that the cRCA aptamers

showed better capturing ability at a higher flow rate (0.1 - 1 mL/h), while the unit aptamer could not handle this increase in flow rate, given that its capturing efficiency dramatically decreased as flow rates increased. Furthermore, it is obvious that the 2 h cRCA aptamer had the best capturing efficiency.

In summary, the optimal condition for this cRCA aptamer-based microfluidic detection system was found to be using the cRCA aptamer modified microchannel synthesized over a reaction time of 2 h, and operated at a flow rate of 0.5 mL/h. In our previous study, the microfluidic detection system was engrafted with unit aptamer and used the flow rate of 0.05 mL/h. In comparison, the sensitivity has been amplified by 10 times while the flow rate of sample injection increased 10-fold as well. This finding is promising given that a high capturing efficiency at a high flow rate is essential to shorten the detection time in real samples [133, 135].

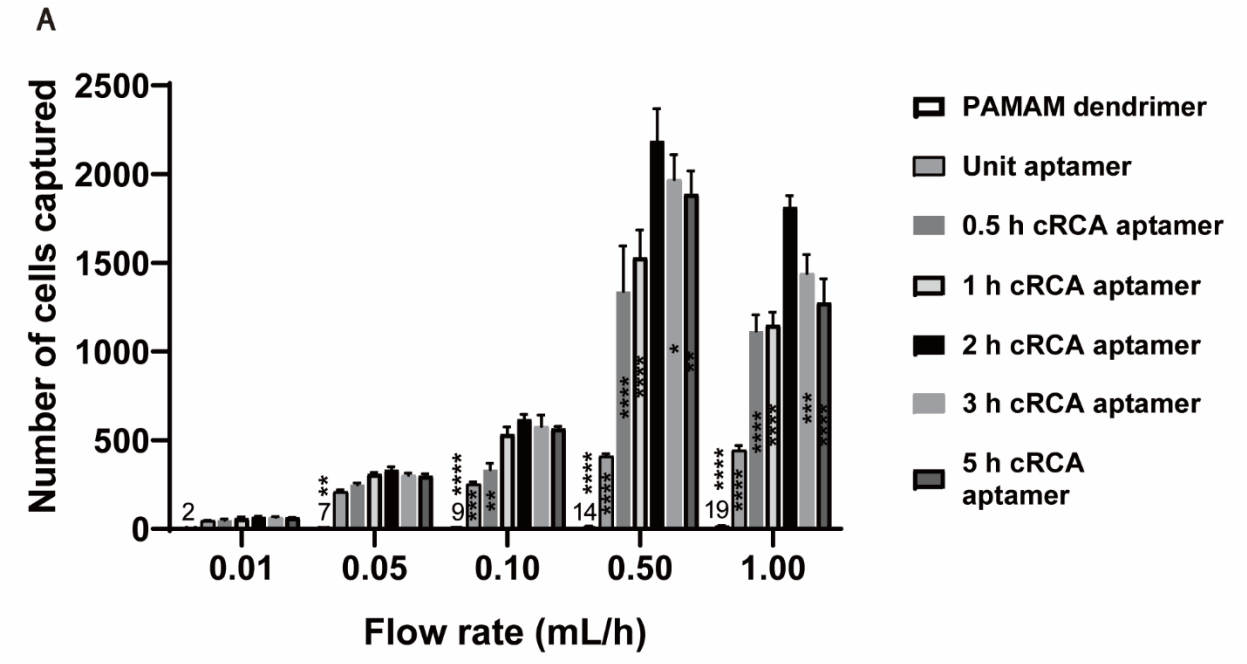

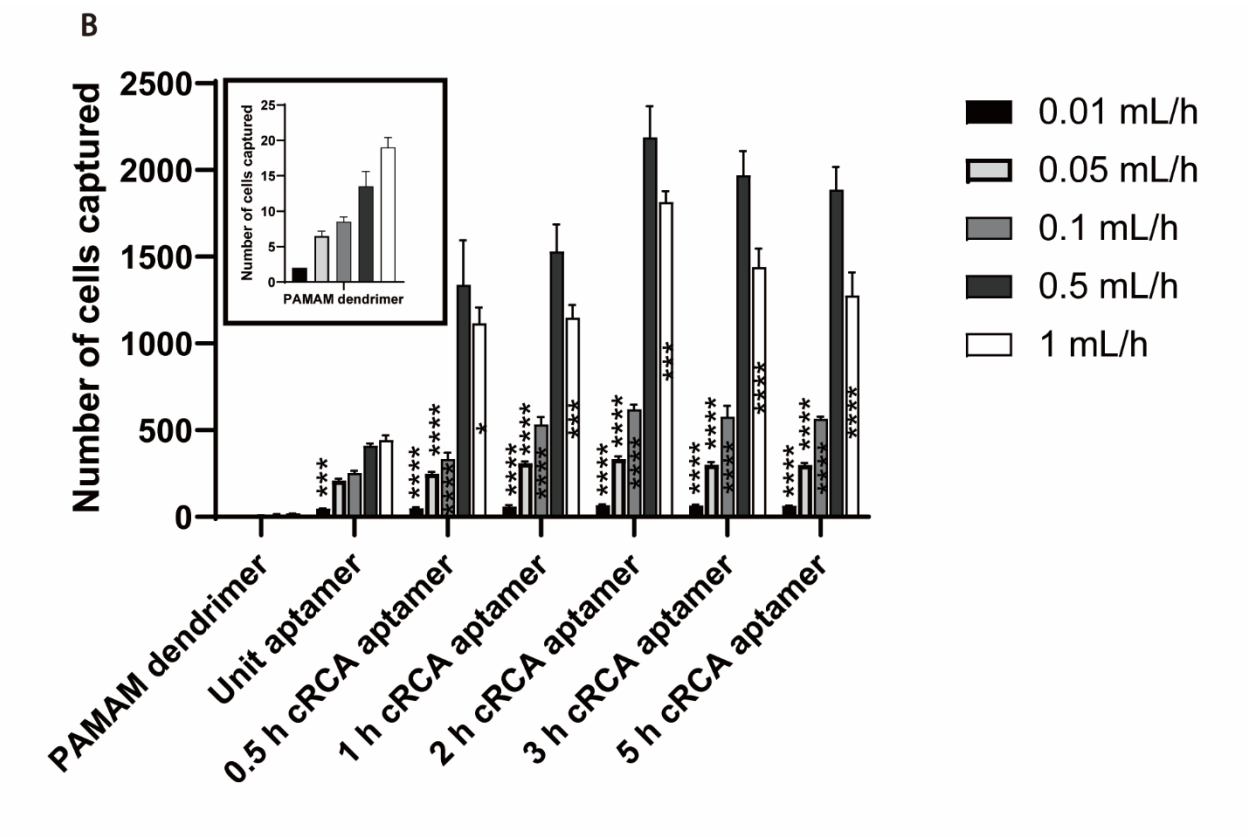
B
Number of cells captured
2500
2000
1500
1000
500
0
Number of cells captured
PAMAM dendrimer
0.01 mL/h
0.05 mL/h
0.1 mL/h
0.5 mL/h
1 mL/h
PAMAM dendrimer
Unit aptamer
0.5 h cRCA aptamer
1 h cRCA aptamer
2 h cRCA aptamer
3 h cRCA aptamer
5 h cRCA aptamer

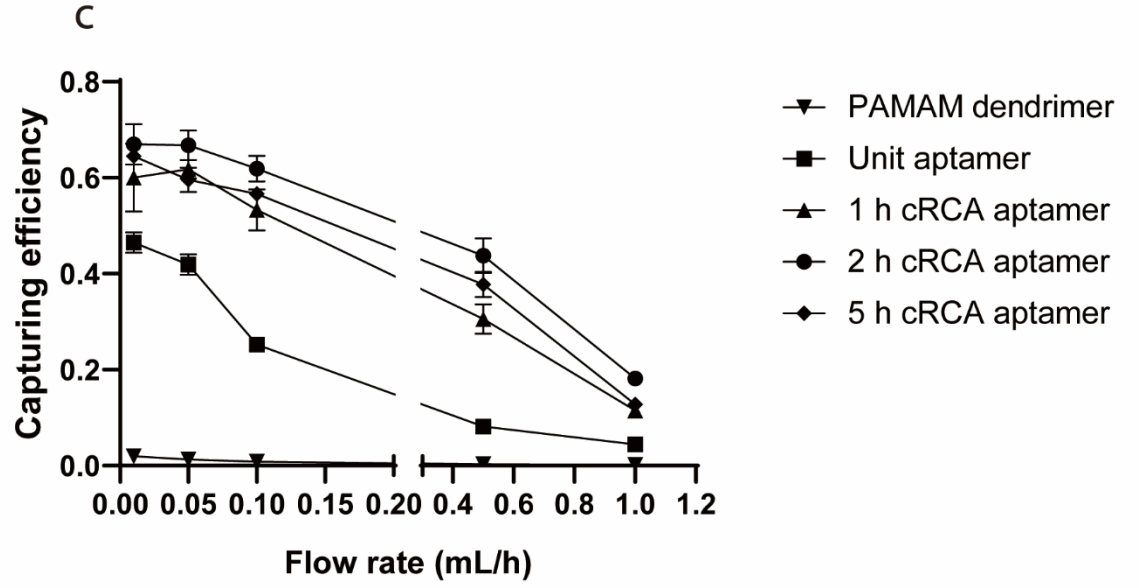
C
Capturing efficiency
0.8
0.6
0.4
0.2
0.0
0.00 0.05 0.10 0.15 0.20 0.4 0.6 0.8 1.0 1.2
Flow rate (mL/h)
PAMAM dendrimer
Unit aptamer
1 h cRCA aptamer
2 h cRCA aptamer
5 h cRCA aptamer

Figure 11. *E. coli* O157:H7 capturing performance of cRCA aptamers modified microchannels under controlled dynamic flow conditions with PAMAM control and unit aptamer comparison. (A) Capturing performance vs. flow rates (B) Capturing performance vs. different aptamers modified microchannels (C) Capturing efficiency vs. flow rates. The microchannel modified by PAMAM dendrimer was used as a control. All experiments were conducted in triplicate. Error bars represent the standard de*via*tions of three measurements.

4.4 AFM images of morphology of cRCA products and structure prediction

All the cRCA products were also characterized by atomic force microscopy. As shown in Figure 12 (A), there were increasing amounts of accumulated cRCA products during the cRCA process. At the first 30 min, there were mostly short strands (40~200 nm), which indicated that the cRCA process was just initiated. The images of the 1 h products showed the elongation of cRCA strands up to 1μm; however, these long chains were not found everywhere. At 2 h, much longer (more than 2 μm) cRCA products appeared and were distributed extensively. The secondary structures of the cRCA products were clearly observed. At 3 h, there was no obvious extension of strands by comparing with that of 2 h cRCA products, and the DNA product tended to entangle instead of extending along a certain direction. Due to the heterogeneous distribution of these cRCA products, there existed the possibility that some inconspicuous areas with longer strands were missed. Also, as time went on, it was difficult to find the start and end points of each strand. Moreover, for the products produced from 5 h amplification, there was a clear DNA network in

the field, and large, condensed structures were present, which may be the condensed enzyme-DNA aggregates [136, 137]. The presence of these aggregated complexes would conceal the capturing structures and may provide a partial explanation for less capturing units observed in the 5 h cRCA products.

Furthermore, the height distribution of 1 h, 2 h and 5 h cRCA products were plotted as Figure 12 (B-D). In the AFM studies of ssDNA and dsDNA, the reported heights varied from 0.3 to 0.6 nm and from 0.7 to 2.0 nm respectively [138-143]. Here, 0.4~0.6 nm and 1.0~1.2 nm were viewed from representative heights of ssDNA and dsDNA individually. By comparing the counts of these two height ranges for these cRCA products, it suggests the ratio of double/single stranded structure increased over time. It is noted that for 1 h and 2 h cRCA products, the height distribution histograms show the unimodal distribution with one peak located at 0.5 nm and 0.6 nm, respectively, which implies that the majority of the population of the cRCA product was single-stranded for the 1 h and 2 h cRCA products. However, for the 5 h cRCA products, the height distribution histogram shows a bimodal distribution with two peaks located at 0.7 nm and 1.2 nm, which indicates that more double-stranded structures had been generated, and these unexpected double-stranded structures were numerous. As a result, capturing structures of the 3 h and 5 h cRCA products changed, leading to a decrease in capturing efficiency as compared to the 2 h cRCA products.

Moreover, the predicted structures of the unit aptamer and several cRCA products at their lowest free energy are shown in Figure 12 (E). There were increasing similar secondary structures of unit aptamer that are found in 10, 20 and 40 copies of cRCA aptamers (*i.e.* the products of 10, 20 and 40 cycles of cRCA reactions), which indicates they can capture greater amount of target cells with increasing cRCA reaction time [144-146]. The prediction of cRCA products implies the fact that the ratio of ssDNA structures and dsDNA structures will not change a lot with the extension of length of the cRCA product. Combining with the results of height distribution histograms, it suggests that extended reaction time introduces more unexpected dsDNA structures, and the presence of dsDNA changes the desired capturing structures unique to the target cell, thus limiting the capturing function of cRCA aptamers [14].

A

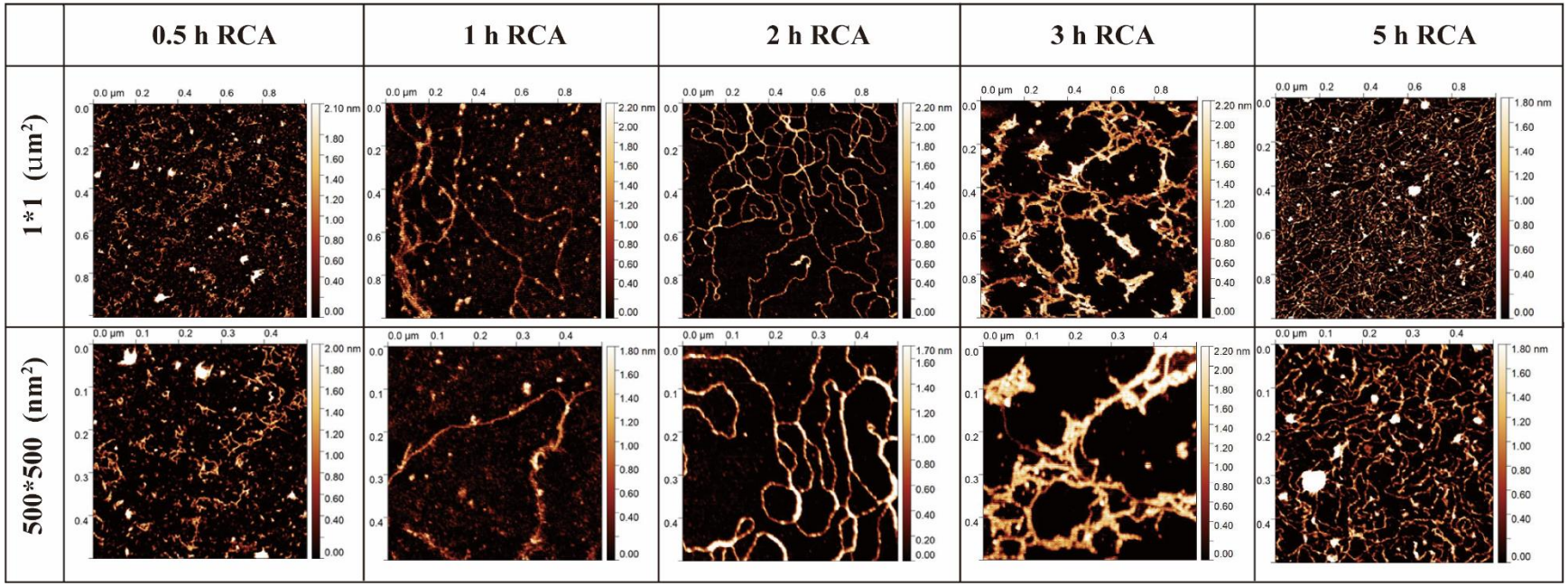

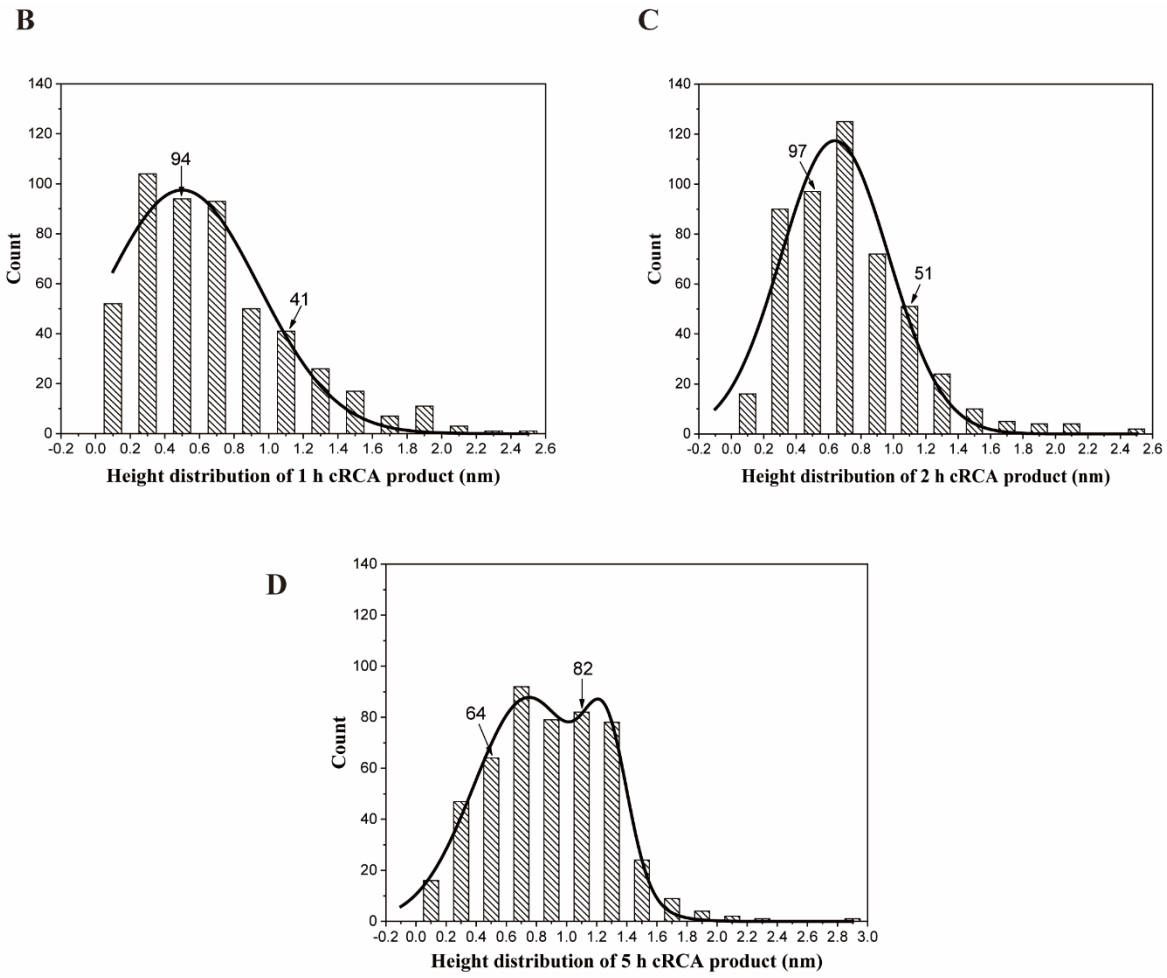
B
C
D
Count
Height distribution of 1 h cRCA product (nm)
Height distribution of 2 h cRCA product (nm)
Height distribution of 5 h cRCA product (nm)
94
41
97
51
64
82

E

Groups	Unit aptamer	cRCA aptamer (10 cycles)
Secondary Structure	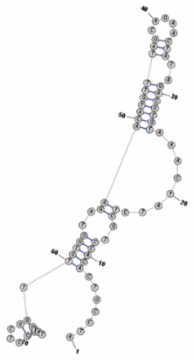	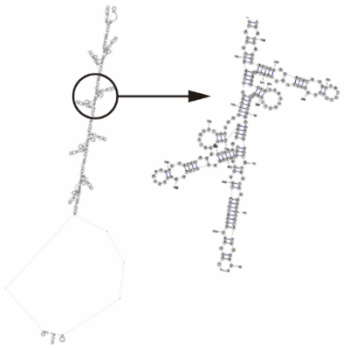
Free Energy (KJ/mol)	-5.5	-107.7

Groups	cRCA aptamer (20 cycles)	cRCA aptamer (40 cycles)
Secondary Structure		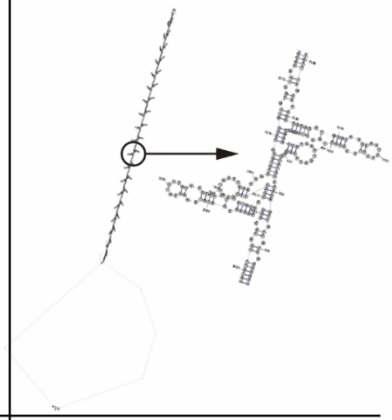
Free Energy (KJ/mol)	-216.7	-434.7

Figure 12. (A) Morphology of cRCA products along reaction time from 0.5 h to 5 h (Dimension: 1μm*1μm; 500nm*500nm); (B) Height distribution of 1 h cRCA products, (C) 2 h cRCA products and (D) 5 h cRCA products (each was counted 500 times in total); (E) Predicted structures of unit aptamer and cRCA products for different cycles of cRCA reaction by software RNA structure 6.0.

4.5 Water contact angle measurement

As shown in Figure 13, the water contact angle of pristine PDMS surface was 115.8±1.1°. After the modification of APTES with O_2 plasma treated PDMS surface, the functionalized surface displayed a water contact angle of 32.8±1.0° [147]. After PAMAM dendrimer was engrafted on PDMS surface, the water contact angle decreased to 19.9±1.6°, which was expected from a previous result [23]. Furthermore, cRCA products grew along the surface for 0.5-5 h, and the water contact angles did not change notably, due to the strong wettability of cRCA products [148, 149], which were 22.3±1.0°, 22.8±1.0°, 21.8±2.3°, 23.5±2.2°, 23.7±1.6° respectively. The water contact angle of each cRCA aptamer modified microchannels did not show any significant difference, which indicates that the reaction time of the RCA process would not generate an impact on the wettability of the inner surface of the cRCA aptamer modified microchannel.

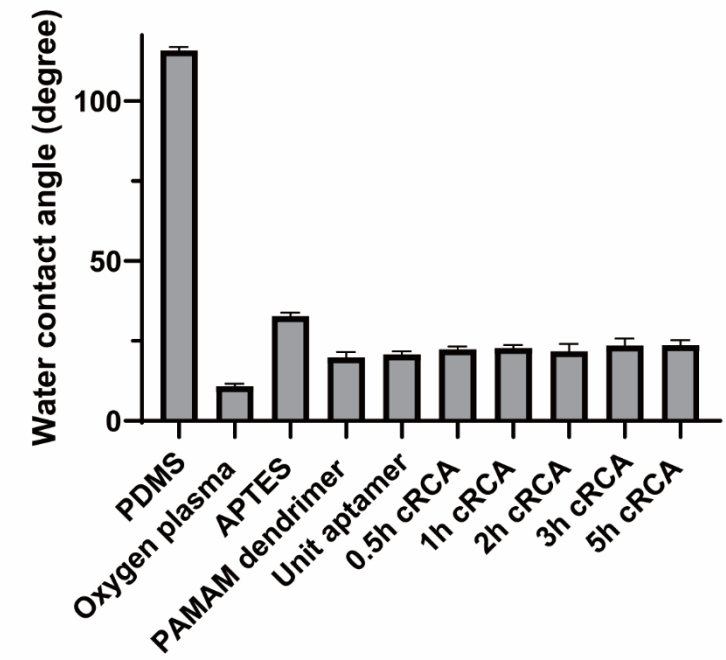

Figure 13. Water contact angle of PDMS surface with different modifications. Each column reported was the average of a minimum of five measurements at separate positions on any given substrate.

4.6 Capturing performance of cRCA aptamer modified microchannel in real sample analysis

Commercially obtained iced tea and bottled water were spiked with *E. coli* O157:H7 cells for real sample analysis. The 2 h cRCA aptamer modified microchannel was used to detect *E. coli* O157:H7 cells in the spiked samples (iced tea, bottled water and PBS solution). For comparison, the unit aptamer modified microchannel was also applied to this analysis, and the PAMAM-COOH modified microchannel was used as a control system for baseline noise. The number of cells captured as a function of $\log_{10}$ [cell concentration (cells/mL)] were plotted, as shown in Figure 14. There was no significant difference between the detection performance in three samples. Also, it is obvious that the numbers of captured cells from all three groups showed increasing trends at cell concentrations ranging from 10^2 to 10^5 cells/mL. By comparing the capturing performance of the differently modified microchannels, the target cells captured by the cRCA aptamer are around 5 times more than the unit aptamer by comparing the slopes of their calibration curves. Since cRCA aptamers contain much more specific capturing units, it is reasonable that the cRCA aptamer-based microchannel exhibited higher capturing efficiency than the unit aptamer-based microchannel. The LOD of the cRCA aptamer modified microchannel was 10^2 cells/mL, which was the same as that of the unit aptamer modified microchannel as reported previously [23, 126].

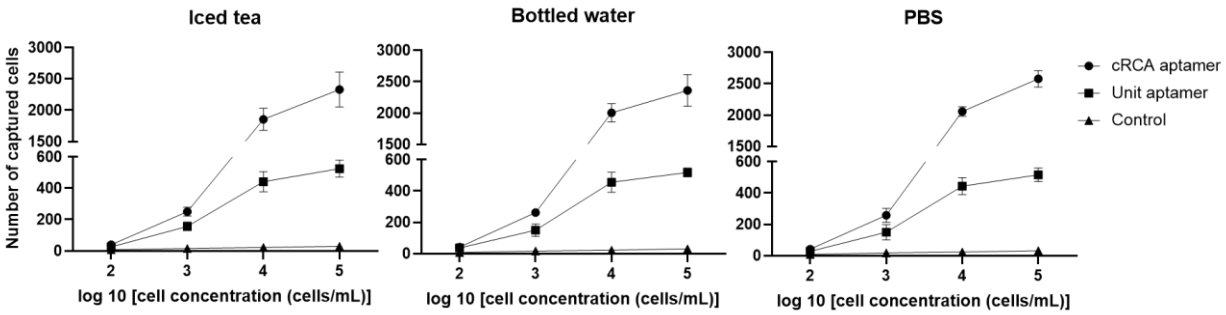

Figure 14. Capturing performance of cRCA aptamer modified microchannel in iced tea, bottled water and PBS spiked with different concentrations (10^2-10^5 cells/mL) of *E. coli* O157:H7 cells. PAMAM-COOH modified microchannel was used as a control system. The flow rate was 0.5 mL/h and the injection time was 1 h. All the experiments were conducted in technical triplicate.

Chapter 5. Conclusion

In this study, optimization of the capturing performance of the cRCA aptamer modified detection system was focused on two factors: the reaction time of the cRCA process, and the flow rate of the sample injected. To pursue the best performance of the cRCA aptamer-based microfluidic detection system, the optimal condition was investigated through an orthogonal experiment with respect to the above two factors. As a result, the design of the cRCA aptamer significantly contributes to an improvement in the capturing performance of the microchannel, and the best capturing performance was achieved when the *in situ* cRCA reaction was carried out for 2 h. Moreover, the capturing performance of this optimized detection system was improved up to 10 times while the throughput was increased 10-fold, compared to our previous unit aptamer-based microfluidic detection system. When the cRCA aptamer modified microchannel was applied to the analysis of real sample, the results also showed good sensitivity as expected which is up to 5 times higher than the unit aptamer modified microchannel.

In addition, a few characterization methods were adopted to explain an unexpected phenomenon that the longer cRCA product (reaction time) does not guarantee a better capturing efficiency, since increasing reaction time may cause more unexpected dsDNA structures to limit the capturing function. Also, the capturing structures of the cRCA aptamer was far more than that of unit aptamer in the unit area of the surface of the microchannel.

Furthermore, the comparison between the detection signal and background noise in iced tea, bottled water and PBS indicated that the LOD of this optimal RCA aptamer-based detection system is 10^2 cells/mL. The excellent performance of cRCA aptamer in iced tea also brings a great advantage to aptamer modified microfluidic system in acidic sample detection. In this study, only

three pure and liquid samples were selected to be test. For detecting some solid substances, the food sample need to be process for further concentration and separation [150]; for some viscous samples which might block the microchannels, introducing bubbles can be used to enhanced the mixing with other liquids [151]; for a larger volume sample, multiple microchannels can be integrated together to form a macroscale device [152].

Chapter 6. Future work

This study suggests that target *E. coli* O157:H7 cells can be specifically detected by cRCA aptamer-based microchannel with a LOD of 10^2 cells/mL. In order to achieve more rapid and sensitive detections, the following projects can be considered in future work.

(1) To develop a dual-RCA based microfluidic system. The current work uses fluorescently labeled *E. coli* O157:H7 cells as the detection target, thus, a signal amplification system is required to be incorporated for real-world detection. In detail, cRCA products would be used to capture the target cells while sRCA products would be used to enhance the detection signals.

(2) To design a staggered herringbone microchannel. The current work uses a straight microchannel for detection. At increased flow rate, the high shear stress limits the capturing efficiency of cRCA aptamer in the microchannel. Therefore, creating a microchannel with inner grooved structures will be useful to overcome this limitation.

References

1. Newell, D.G., et al., *Food-borne diseases—the challenges of 20 years ago still persist while new ones continue to emerge.* International journal of food microbiology, 2010. **139**: p. S3-S15.
2. Rangel, J.M., et al., *Epidemiology of Escherichia coli O157: H7 outbreaks, united states, 1982–2002.* Emerging infectious diseases, 2005. **11**(4): p. 603.
3. Canada, P.H.A.o. *Outbreak of E. coli infections linked to romaine lettuce*. 2018; Available from: https://www.canada.ca/en/public-health/services/public-health-notices/2018/public-health-notice-outbreak-e-coli-infections-linked-romaine-lettuce.html.
4. Mandal, P., et al., *Methods for rapid detection of foodborne pathogens: an overview.* American Journal Of Food Technology, 2011. **6**(2): p. 87-102.
5. Gracias, K.S. and J.L. McKillip, *A review of conventional detection and enumeration methods for pathogenic bacteria in food.* Canadian journal of microbiology, 2004. **50**(11): p. 883-890.
6. Croxen, M.A., et al., *Recent advances in understanding enteric pathogenic Escherichia coli.* Clinical microbiology reviews, 2013. **26**(4): p. 822-880.
7. Carey-Ann, B.D. and K.C. Carroll, *Diagnosis of Clostridium difficile infection: an ongoing conundrum for clinicians and for clinical laboratories.* Clinical microbiology reviews, 2013. **26**(3): p. 604-630.
8. Ahmed, A., et al., *Biosensors for whole-cell bacterial detection.* Clinical microbiology reviews, 2014. **27**(3): p. 631-646.
9. Yoon, J.-Y. and B. Kim, *Lab-on-a-chip pathogen sensors for food safety.* Sensors, 2012. **12**(8): p. 10713-10741.
10. Arora, P., et al., *Biosensors as innovative tools for the detection of food borne pathogens.* Biosensors and Bioelectronics, 2011. **28**(1): p. 1-12.
11. Jiang, Y., S. Zou, and X. Cao, *Rapid and ultra-sensitive detection of foodborne pathogens by using miniaturized microfluidic devices: a review.* Analytical Methods, 2016. **8**(37): p. 6668-6681.
12. Wu, W., et al., *An aptamer-based biosensor for colorimetric detection of Escherichia coli O157: H7.* PloS one, 2012. **7**(11): p. e48999.
13. Yan, X., et al., *Highly sensitive fluorescent aptasensor for Salmonella paratyphi A via DNase I-mediated cyclic signal amplification.* Analytical Methods, 2015. **7**(24): p. 10243-10250.
14. Zhao, W., et al., *Bioinspired multivalent DNA network for capture and release of cells.* Proceedings of the National Academy of Sciences, 2012. **109**(48): p. 19626-19631.
15. Zhang, Z., et al., *A polyvalent aptamer system for targeted drug delivery.* Biomaterials, 2013. **34**(37): p. 9728-9735.
16. Tang, J., et al., *Polyvalent and thermosensitive DNA nanoensembles for cancer cell detection and manipulation.* Analytical chemistry, 2017. **89**(12): p. 6637-6644.
17. Jiang, Y., et al., *Rolling circle amplification and its application in microfluidic systems for Escherichia coli O157:H7 detections.* Journal of Food Safety. **0**(0): p. e12671.
18. Takahashi, H., Y. Okamura, and T. Kobori, *Use of DNA CircLigase for Direct Isothermal Detection of Microbial mRNAs by RNA-Primed Rolling Circle Amplification and Preparation of ø29 DNA Polymerase Not Contaminated by Amplifiable DNA*, in *Rolling circle amplification (RCA)*. 2016, Springer. p. 37-46.
19. Poltronieri, P., et al., *Biosensors for the detection of food pathogens.* Foods, 2014. **3**(3): p. 511-526.

20. Zhou, L., et al., *Aptamer-based rolling circle amplification: a platform for electrochemical detection of protein.* Analytical chemistry, 2007. **79**(19): p. 7492-7500.

21. Ma, C., et al., *Cocaine detection via rolling circle amplification of short DNA strand separated by magnetic beads.* Biosensors and Bioelectronics, 2011. **26**(7): p. 3309-3312.

22. Gu, L., et al., *Research progress on rolling circle amplification (RCA)-based biomedical sensing.* Pharmaceuticals, 2018. **11**(2): p. 35.

23. Hao, X., et al., *Aptamer surface functionalization of microfluidic devices using dendrimers as multi-handled templates and its application in sensitive detections of foodborne pathogenic bacteria.* Analytica chimica acta, 2019. **1056**: p. 96-107.

24. Qin, Y., et al., *Developing an ultra non-fouling SU-8 and PDMS hybrid microfluidic device by poly (amidoamine) engraftment.* Colloids and Surfaces B: Biointerfaces, 2015. **127**: p. 247-255.

25. CDC. *Reports of Selected E. coli Outbreak Investigations*. 2019; Available from: https://www.cdc.gov/ecoli/outbreaks.html.

26. Roos, V., et al., *The asymptomatic bacteriuria Escherichia coli strain 83972 outcompetes uropathogenic E. coli strains in human urine.* Infection and immunity, 2006. **74**(1): p. 615-624.

27. Tilden Jr, J., et al., *A new route of transmission for Escherichia coli: infection from dry fermented salami.* American journal of public health, 1996. **86**(8_Pt_1): p. 1142-1145.

28. Diez-Gonzalez, F., et al., *Grain feeding and the dissemination of acid-resistant Escherichia coli from cattle.* Science, 1998. **281**(5383): p. 1666-1668.

29. Besser, T., et al., *Escherichia coli O157 [ratio] H7 infection of calves: infectious dose and direct contact transmission.* Epidemiology & Infection, 2001. **127**(3): p. 555-560.

30. March, S.B. and S. Ratnam, *Sorbitol-MacConkey medium for detection of Escherichia coli O157: H7 associated with hemorrhagic colitis.* Journal of clinical microbiology, 1986. **23**(5): p. 869-872.

31. Inoue, K., et al., *Evaluation of L-pyrrolidonyl peptidase paper strip test for differentiation of members of the family Enterobacteriaceae, particularly Salmonella spp.* Journal of clinical microbiology, 1996. **34**(7): p. 1811-1812.

32. Duffy, G., et al., *A membrane-immunofluorescent-viability staining technique for the detection of Salmonella spp. from fresh and processed meat samples.* Journal of applied microbiology, 2000. **89**(4): p. 587-594.

33. Sunwoo, H.H., W.W. Wang, and J.S. Sim, *Detection of Escherichia coli O157: H7 using chicken immunoglobulin Y.* Immunology letters, 2006. **106**(2): p. 191-193.

34. Deisingh, A.K. and M. Thompson, *Detection of infectious and toxigenic bacteria.* Analyst, 2002. **127**(5): p. 567-581.

35. Silk, T.M. and C.W. Donnelly, *Increased detection of acid-injured Escherichia coli O157: H7 in autoclaved apple cider by using nonselective repair on trypticase soy agar.* Journal of food protection, 1997. **60**(12): p. 1483-1486.

36. Doyle, M.P. and J.L. Schoeni, *Isolation of Escherichia coli O157: H7 from retail fresh meats and poultry.* Appl. Environ. Microbiol., 1987. **53**(10): p. 2394-2396.

37. Blais, B., et al., *Comparison of fluorogenic and chromogenic assay systems in the detection of Escherichia coli O157 by a novel polymyxin-based ELISA.* Letters in applied microbiology, 2004. **39**(6): p. 516-522.

38. Sapsford, K.E., et al., *Detection of Campylobacter and Shigella species in food samples using an array biosensor.* Analytical chemistry, 2004. **76**(2): p. 433-440.

39. Seo, K., et al., *Immunomagnetic separation and flow cytometry for rapid detection of Escherichia coli O157: H7.* Journal of food protection, 1998. **61**(7): p. 812-816.

40. Yamaguchi, N., et al., *Rapid detection of respiring Escherichia coli O157: H7 in apple juice, milk, and ground beef by flow cytometry.* Cytometry Part A: the journal of the International Society for Analytical Cytology, 2003. **54**(1): p. 27-35.

41. Fratamico, P.M., et al., *Detection of Escherichia coli O157: H7 by multiplex PCR.* Journal of Clinical Microbiology, 1995. **33**(8): p. 2188-2191.

42. Ibekwe, A.M., et al., *Multiplex fluorogenic real-time PCR for detection and quantification of Escherichia coli O157: H7 in dairy wastewater wetlands.* Appl. Environ. Microbiol., 2002. **68**(10): p. 4853-4862.

43. DeMarco, D.R., et al., *Rapid detection of Escherichia coli O157: H7 in ground beef using a fiber-optic biosensor.* Journal of food protection, 1999. **62**(7): p. 711-716.

44. Ohk, S.-H. and A.K. Bhunia, *Multiplex fiber optic biosensor for detection of Listeria monocytogenes, Escherichia coli O157: H7 and Salmonella enterica from ready-to-eat meat samples.* Food microbiology, 2013. **33**(2): p. 166-171.

45. Gfeller, K.Y., N. Nugaeva, and M. Hegner, *Micromechanical oscillators as rapid biosensor for the detection of active growth of Escherichia coli.* Biosensors and Bioelectronics, 2005. **21**(3): p. 528-533.

46. Brigati, J.R., et al., *Bacteriophage-based bioluminescent bioreporter for the detection of Escherichia coli O157: H7.* Journal of food protection, 2007. **70**(6): p. 1386-1392.

47. Wu, W., et al., *A sensitive lateral flow biosensor for Escherichia coli O157: H7 detection based on aptamer mediated strand displacement amplification.* Analytica chimica acta, 2015. **861**: p. 62-68.

48. Brosel-Oliu, S., et al., *Novel impedimetric aptasensor for label-free detection of Escherichia coli O157: H7.* Sensors and Actuators B: Chemical, 2018. **255**: p. 2988-2995.

49. Varshney, M., et al., *A label-free, microfluidics and interdigitated array microelectrode-based impedance biosensor in combination with nanoparticles immunoseparation for detection of Escherichia coli O157: H7 in food samples.* Sensors and Actuators B: Chemical, 2007. **128**(1): p. 99-107.

50. Subramanian, A., J. Irudayaraj, and T. Ryan, *A mixed self-assembled monolayer-based surface plasmon immunosensor for detection of E. coli O157: H7.* Biosensors and Bioelectronics, 2006. **21**(7): p. 998-1006.

51. Gu, J., et al., *Enhancement of the sensitivity of surface plasmon resonance biosensor with colloidal gold labeling technique.* Supramolecular Science, 1998. **5**(5-6): p. 695-698.

52. Huang, C.-J., et al., *Long-range surface plasmon-enhanced fluorescence spectroscopy biosensor for ultrasensitive detection of E. coli O157: H7.* Analytical Chemistry, 2011. **83**(3): p. 674-677.

53. Progatzky, F., M.J. Dallman, and C. Lo Celso, *From seeing to believing: labelling strategies for in vivo cell-tracking experiments.* Interface focus, 2013. **3**(3): p. 20130001.

54. Goodridge, L., J. Chen, and M. Griffiths, *The use of a fluorescent bacteriophage assay for detection of Escherichia coli O157: H7 in inoculated ground beef and raw milk.* International journal of food microbiology, 1999. **47**(1-2): p. 43-50.

55. Hendrickson, O.D., et al., *Lectin-based detection of Escherichia coli and Staphylococcus aureus by flow cytometry.* Archives of microbiology, 2019. **201**(3): p. 313-324.

56. Dhull, N., et al., *Label-free amperometric biosensor for Escherichia coli O157: H7 detection.* Applied Surface Science, 2019. **495**: p. 143548.

57. Priyanka, B., R.K. Patil, and S. Dwarakanath, *A review on detection methods used for foodborne pathogens.* The Indian journal of medical research, 2016. **144**(3): p. 327.

58. Melin, J. and S.R. Quake, *Microfluidic large-scale integration: the evolution of design rules for biological automation.* Annu. Rev. Biophys. Biomol. Struct., 2007. **36**: p. 213-231.

59. Singh, R., et al., *Biosensors for pathogen detection: A smart approach towards clinical diagnosis.* Sensors and Actuators B: Chemical, 2014. **197**: p. 385-404.

60. Heo, J. and S.Z. Hua, *An overview of recent strategies in pathogen sensing.* Sensors, 2009. **9**(6): p. 4483-4502.

61. Atalay, Y.T., et al., *Microfluidic analytical systems for food analysis.* Trends in food science & technology, 2011. **22**(7): p. 386-404.

62. Mazaafrianto, D., et al., *Recent microdevice-based Aptamer sensors.* Micromachines, 2018. **9**(5): p. 202.

63. Bubendorfer, A., X. Liu, and A.V. Ellis, *Microfabrication of PDMS microchannels using SU-8/PMMA moldings and their sealing to polystyrene substrates.* Smart Materials and Structures, 2007. **16**(2): p. 367.

64. Gaso, M., et al., *Love wave biosensors: a review.* State of the art in biosensors-general aspects, InTech., 2013: p. 277-310.

65. Niu, Z.Q., et al., *DNA amplification on a PDMS–glass hybrid microchip.* Journal of micromechanics and microengineering, 2006. **16**(2): p. 425.

66. McDonald, J.C., et al., *Fabrication of microfluidic systems in poly (dimethylsiloxane).* ELECTROPHORESIS: An International Journal, 2000. **21**(1): p. 27-40.

67. Goddard, J.M. and J. Hotchkiss, *Polymer surface modification for the attachment of bioactive compounds.* Progress in polymer science, 2007. **32**(7): p. 698-725.

68. Eteshola, E. and D. Leckband, *Development and characterization of an ELISA assay in PDMS microfluidic channels.* Sensors and Actuators B: Chemical, 2001. **72**(2): p. 129-133.

69. Yamada, M. and M. Seki, *Nanoliter-sized liquid dispenser array for multiple biochemical analysis in microfluidic devices.* Analytical chemistry, 2004. **76**(4): p. 895-899.

70. Ross, D., M. Gaitan, and L.E. Locascio, *Temperature measurement in microfluidic systems using a temperature-dependent fluorescent dye.* Analytical chemistry, 2001. **73**(17): p. 4117-4123.

71. Seguin, C., et al., *Surface modification of poly (dimethylsiloxane) for microfluidic assay applications.* Applied Surface Science, 2010. **256**(8): p. 2524-2531.

72. Zhou, J., A.V. Ellis, and N.H. Voelcker, *Recent developments in PDMS surface modification for microfluidic devices.* Electrophoresis, 2010. **31**(1): p. 2-16.

73. Zhou, J., et al., *Surface modification for PDMS-based microfluidic devices.* Electrophoresis, 2012. **33**(1): p. 89-104.

74. Esfand, R. and D.A. Tomalia, *Poly (amidoamine)(PAMAM) dendrimers: from biomimicry to drug delivery and biomedical applications.* Drug discovery today, 2001. **6**(8): p. 427-436.

75. Qin, Y., *Developing a poly (dimethylsiloxane)(PDMS)/SU-8 (negative photoresist) hybrid microfluidic system for sensitive detection of circulating tumour cells*. 2018, Université d'Ottawa/University of Ottawa.

76. Abbasi, E., et al., *Dendrimers: synthesis, applications, and properties*. Nanoscale research letters, 2014. **9**(1): p. 247.

77. Yiyun, C., et al., *Transdermal delivery of nonsteroidal anti-inflammatory drugs mediated by polyamidoamine (PAMAM) dendrimers.* Journal of pharmaceutical sciences, 2007. **96**(3): p. 595-602.

78. Jayasena, S.D., *Aptamers: an emerging class of molecules that rival antibodies in diagnostics.* Clinical chemistry, 1999. **45**(9): p. 1628-1650.

79. Mujika, M., et al., *Magnetoresistive immunosensor for the detection of Escherichia coli O157: H7 including a microfluidic network.* Biosensors and Bioelectronics, 2009. **24**(5): p. 1253-1258.

80. Pal, S., E.C. Alocilja, and F.P. Downes, *Nanowire labeled direct-charge transfer biosensor for detecting Bacillus species.* Biosensors and Bioelectronics, 2007. **22**(9-10): p. 2329-2336.

81. Delehanty, J.B. and F.S. Ligler, *A microarray immunoassay for simultaneous detection of proteins and bacteria.* Analytical Chemistry, 2002. **74**(21): p. 5681-5687.

82. Self, C.H. and D.B. Cook, *Advances in immunoassay technology.* Current opinion in biotechnology, 1996. **7**(1): p. 60-65.

83. Shaughnessy, A.F., *Monoclonal antibodies: magic bullets with a hefty price tag.* Bmj, 2012. **345**: p. e8346.

84. Dráber, P., E. Dráberová, and M. Nováková, *Stability of monoclonal IgM antibodies freeze-dried in the presence of trehalose.* Journal of immunological methods, 1995. **181**(1): p. 37-43.

85. Cox, J.C., P. Rudolph, and A.D. Ellington, *Automated RNA selection.* Biotechnology progress, 1998. **14**(6): p. 845-850.

86. Jenison, R.D., et al., *High-resolution molecular discrimination by RNA.* Science, 1994. **263**(5152): p. 1425-1429.

87. Wang, T., et al., *Three decades of nucleic acid aptamer technologies: Lessons learned, progress and opportunities on aptamer development.* Biotechnology advances, 2018.

88. Wang, T., et al., *EpCAM aptamer-mediated survivin silencing sensitized cancer stem cells to doxorubicin in a breast cancer model.* Theranostics, 2015. **5**(12): p. 1456.

89. Xu, Y., X. Yang, and E. Wang, *Aptamers in microfluidic chips.* Analytica chimica acta, 2010. **683**(1): p. 12-20.

90. Morrissey, D.V., et al., *Activity of stabilized short interfering RNA in a mouse model of hepatitis B virus replication.* Hepatology, 2005. **41**(6): p. 1349-1356.

91. Dass, C.R., et al., *Cellular uptake, distribution, and stability of 10-23 deoxyribozymes.* Antisense and Nucleic Acid Drug Development, 2002. **12**(5): p. 289-299.

92. Ni, S., et al., *Chemical modifications of nucleic acid aptamers for therapeutic purposes.* International journal of molecular sciences, 2017. **18**(8): p. 1683.

93. ORTIGAO, J.R., et al., *Oligonucleotide analogs with terminal 3', 3'-and 5', 5'-internucleotidic linkages as antisense inhibitors of viral replication.* Antisense Research and Development, 1991. **1**(4): p. 380-380.

94. Shum, K.T. and J.A. Tanner, *Differential inhibitory activities and stabilisation of DNA aptamers against the SARS coronavirus helicase.* Chembiochem, 2008. **9**(18): p. 3037-3045.

95. Dougan, H., et al., *Extending the lifetime of anticoagulant oligodeoxynucleotide aptamers in blood.* Nuclear medicine and biology, 2000. **27**(3): p. 289-297.

96. Ruckman, J., et al., *2'-Fluoropyrimidine RNA-based aptamers to the 165-amino acid form of vascular endothelial growth factor (VEGF165) Inhibition of receptor binding and VEGF-induced vascular permeability through interactions requiring the exon 7-encoded domain.* Journal of Biological Chemistry, 1998. **273**(32): p. 20556-20567.

97. Ng, E.W., et al., *Pegaptanib, a targeted anti-VEGF aptamer for ocular vascular disease.* Nature reviews drug discovery, 2006. **5**(2): p. 123.

98. Lee, C.H., et al., *Pharmacokinetics of a cholesterol-conjugated aptamer against the hepatitis C virus (HCV) NS5B protein.* Molecular Therapy-Nucleic Acids, 2015. **4**: p. e254.

99. Willis, M.C., et al., *Liposome-anchored vascular endothelial growth factor aptamers.* Bioconjugate chemistry, 1998. **9**(5): p. 573-582.

100. Green, L.S., et al., *Nuclease-resistant nucleic acid ligands to vascular permeability factor/vascular endothelial growth factor.* Chemistry & biology, 1995. **2**(10): p. 683-695.

101. Abeydeera, N.D., et al., *Evoking picomolar binding in RNA by a single phosphorodithioate linkage.* Nucleic acids research, 2016. **44**(17): p. 8052-8064.

102. Rohloff, J.C., et al., *Nucleic acid ligands with protein-like side chains: modified aptamers and their use as diagnostic and therapeutic agents.* Molecular Therapy-Nucleic Acids, 2014. **3**: p. e201.

103. So, H.-M., et al., *Single-walled carbon nanotube biosensors using aptamers as molecular recognition elements.* Journal of the American Chemical Society, 2005. **127**(34): p. 11906-11907.

104. Obubuafo, A., et al., *Poly (methyl methacrylate) microchip affinity capillary gel electrophoresis of aptamer–protein complexes for the analysis of thrombin in plasma.* Electrophoresis, 2008. **29**(16): p. 3436-3445.

105. Xu, Y., et al., *Aptamer-based microfluidic device for enrichment, sorting, and detection of multiple cancer cells.* Analytical chemistry, 2009. **81**(17): p. 7436-7442.

106. Ali, M.M., et al., *Rolling circle amplification: a versatile tool for chemical biology, materials science and medicine.* Chem Soc Rev, 2014. **43**(10): p. 3324-41.

107. Akter, F., et al., *Detection of antigens using a protein–DNA chimera developed by enzymatic covalent bonding with phiX gene A.* Analytical chemistry, 2012. **84**(11): p. 5040-5046.

108. Yang, L., et al., *Real-Time Rolling Circle Amplification for Protein Detection.* Analytical Chemistry, 2007. **79**(9): p. 3320-3329.

109. Ou, L.-J., et al., *DNA encapsulating liposome based rolling circle amplification immunoassay as a versatile platform for ultrasensitive detection of protein.* Analytical chemistry, 2009. **81**(23): p. 9664-9673.

110. Gyanchandani, R., et al., *Whole genome amplification of cell-free DNA enables detection of circulating tumor DNA mutations from fingerstick capillary blood.* Scientific Reports, 2018. **8**(1): p. 17313.

111. Qi, X., et al., *L-RCA (ligation-rolling circle amplification): a general method for genotyping of single nucleotide polymorphisms (SNPs).* Nucleic acids research, 2001. **29**(22): p. E116-E116.

112. Yao, M., et al., *Specific and simultaneous detection of micro RNA 21 and let-7a by rolling circle amplification combined with lateral flow strip.* Analytica Chimica Acta, 2018.

113. Jiang, Y., S. Zou, and X. Cao, *A simple dendrimer-aptamer based microfluidic platform for E. coli O157:H7 detection and signal intensification by rolling circle amplification.* Sensors and Actuators B: Chemical, 2017. **251**: p. 976-984.

114. Gu, L., et al., *Research Progress on Rolling Circle Amplification (RCA)-Based Biomedical Sensing.* Pharmaceuticals (Basel), 2018. **11**(2).

115. Cosnier, S. and P. Mailley, *Recent advances in DNA sensors.* Analyst, 2008. **133**(8): p. 984-991.

116. Li, J., et al., *Rolling Circle Amplification Combined with Gold Nanoparticle Aggregates for Highly Sensitive Identification of Single-Nucleotide Polymorphisms.* Analytical Chemistry, 2010. **82**(7): p. 2811-2816.

117. Zhao, W., et al., *DNA polymerization on gold nanoparticles through rolling circle amplification: towards novel scaffolds for three-dimensional periodic nanoassemblies.* Angewandte Chemie International Edition, 2006. **45**(15): p. 2409-2413.

118. Cheglakov, Z., et al., *Increasing the complexity of periodic protein nanostructures by the rolling-circle-amplified synthesis of aptamers.* Angew Chem Int Ed Engl, 2008. **47**(1): p. 126-30.

119. Joffroy, B., et al., *Rolling circle amplification shows a sinusoidal template length-dependent amplification bias.* Nucleic acids research, 2018. **46**(2): p. 538-545.

120. Mao, Y., et al., *Optimal DNA templates for rolling circle amplification revealed by in vitro selection.* Chemistry, 2015. **21**(22): p. 8069-74.

121. de Vega, M., et al., *Improvement of φ29 DNA polymerase amplification performance by fusion of DNA binding motifs.* Proceedings of the National Academy of Sciences of the United States of America, 2010. **107**(38): p. 16506-16511.

122. Cui, Y., et al., *Terminal hairpin in oligonucleotide dominantly prioritizes intramolecular cyclization by T4 ligase over intermolecular polymerization: an exclusive methodology for producing ssDNA rings.* Nucleic Acids Res, 2018. **46**(22): p. e132.

123. Inoue, J., Y. Shigemori, and T. Mikawa, *Improvements of rolling circle amplification (RCA) efficiency and accuracy using Thermus thermophilus SSB mutant protein.* Nucleic Acids Res, 2006. **34**(9): p. e69.

124. Liu, Q., et al., *Improvement of rolling circle amplification efficiency with gold nanoparticles.* Materials Research Innovations, 2015. **19**(sup9): p. S9-337-S9-339.

125. Bruno, J.G. and J. Chanpong, *Methods of producing competitive aptamer fret reagents and assays*. 2009, Google Patents.

126. Jiang, Y., S. Zou, and X. Cao, *A simple dendrimer-aptamer based microfluidic platform for E. coli O157:H7 detection and signal intensification by rolling circle amplification.* Sensors and Actuators B: Chemical, 2017. **251**(Supplement C): p. 976-984.

127. Qin, D., Y. Xia, and G.M. Whitesides, *Soft lithography for micro-and nanoscale patterning.* Nature protocols, 2010. **5**(3): p. 491.

128. Yeh, P.Y., et al., *Nonfouling hydrophilic poly(ethylene glycol) engraftment strategy for PDMS/SU-8 heterogeneous microfluidic devices.* Langmuir, 2012. **28**(46): p. 16227-36.

129. Ouellet, E., et al., *Novel Carboxyl-Amine Bonding Methods for Poly(dimethylsiloxane)-Based Devices.* Langmuir, 2010. **26**(14): p. 11609-11614.

130. Zuker, M., *Calculating nucleic acid secondary structure.* Current opinion in structural biology, 2000. **10**(3): p. 303-310.

131. Mathews, D.H. and D.H. Turner, *Prediction of RNA secondary structure by free energy minimization.* Current opinion in structural biology, 2006. **16**(3): p. 270-278.

132. Xu, Z.Z. and D.H. Mathews, *Secondary structure prediction of single sequences using RNAstructure*, in *RNA Structure Determination*. 2016, Springer. p. 15-34.

133. Zhang, J., W. Sheng, and Z.H. Fan, *An ensemble of aptamers and antibodies for multivalent capture of cancer cells.* Chemical Communications, 2014. **50**(51): p. 6722-6725.

134. Wan, Y., et al., *Capture, isolation and release of cancer cells with aptamer-functionalized glass bead array.* Lab on a Chip, 2012. **12**(22): p. 4693-4701.

135. Nagrath, S., et al., *Isolation of rare circulating tumour cells in cancer patients by microchip technology.* Nature, 2007. **450**: p. 1235.

136. Peeters, E., et al., *DNA-interacting characteristics of the archaeal rudiviral protein SIRV2_Gp1.* Viruses, 2017. **9**(7): p. 190.

137. Moreno-Herrero, F., et al., *Atomic force microscopy shows that vaccinia topoisomerase IB generates filaments on DNA in a cooperative fashion.* Nucleic acids research, 2005. **33**(18): p. 5945-5953.

138. Becerril, H.A., et al., *Ionic surface masking for low background in single-and double-stranded DNA-templated silver and copper nanorods.* Journal of Materials Chemistry, 2004. **14**(4): p. 611-616.

139. Brett, A.M.O. and A.-M.C. Paquim, *DNA imaged on a HOPG electrode surface by AFM with controlled potential.* Bioelectrochemistry, 2005. **66**(1-2): p. 117-124.

140. Hansma, H.G., et al., *Atomic force microscopy of long and short double-stranded, single-stranded and triple-stranded nucleic acids.* Nucleic acids research, 1996. **24**(4): p. 713-720.

141. Kotlyar, A.B., et al., *Long, monomolecular guanine-based nanowires.* Advanced Materials, 2005. **17**(15): p. 1901-1905.

142. Wang, H., et al., *Self-assembled monolayer of ssDNA on Au (1 1 1) substrate.* Surface science, 2001. **480**(1-2): p. L389-L394.

143. Adamcik, J., et al., *Observation of single-stranded DNA on mica and highly oriented pyrolytic graphite by atomic force microscopy.* FEBS letters, 2006. **580**(24): p. 5671-5675.

144. Wu, W., et al., *An aptamer-based biosensor for colorimetric detection of Escherichia coli O157:H7.* PLoS One, 2012. **7**(11): p. e48999.

145. Xie, P., et al., *Highly sensitive detection of lipopolysaccharides using an aptasensor based on hybridization chain reaction.* Sci Rep, 2016. **6**: p. 29524.

146. Lee, Y.J., et al., *In vitro selection of Escherichia coli O157:H7-specific RNA aptamer.* Biochem Biophys Res Commun, 2012. **417**(1): p. 414-20.

147. Zhu, Z., et al., *A versatile bonding method for PDMS and SU-8 and its application towards a multifunctional microfluidic device.* Micromachines, 2016. **7**(12): p. 230.

148. Tian, Q., et al., *Carbon nanotube enhanced label-free detection of microRNAs based on hairpin probe triggered solid-phase rolling-circle amplification.* Nanoscale, 2015. **7**(3): p. 987-993.

149. Chrisey, L.A., G.U. Lee, and C.E. O'Ferrall, *Covalent attachment of synthetic DNA to self-assembled monolayer films.* Nucleic acids research, 1996. **24**(15): p. 3031-3039.

150. Beebe, D.J., G.A. Mensing, and G.M. Walker, *Physics and applications of microfluidics in biology.* Annual review of biomedical engineering, 2002. **4**(1): p. 261-286.

151. Yaralioglu, G.G., et al., *Ultrasonic mixing in microfluidic channels using integrated transducers.* Analytical chemistry, 2004. **76**(13): p. 3694-3698.

152. Neethirajan, S., et al., *Microfluidics for food, agriculture and biosystems industries.* Lab on a Chip, 2011. **11**(9): p. 1574-1586.

Appendix

Table S1. Two-way ANOVA test of multiple comparison of capturing performance between arbitrary two modified microchannels at controlled flow rates (α= 0.05), which was obtained from Graphpad software (ns means not significant).

Tukey's multiple comparisons test	Significant?	Summary	Adjusted P Value
0.01 mL/h			
PAMAM dendrimer vs. Unit aptamer	No	ns	0.9974
PAMAM dendrimer vs. 0.5 h cRCA aptamer	No	ns	0.9965
PAMAM dendrimer vs. 1 h cRCA aptamer	No	ns	0.9892
PAMAM dendrimer vs. 2 h cRCA aptamer	No	ns	0.9805
PAMAM dendrimer vs. 3 h cRCA aptamer	No	ns	0.9834
PAMAM dendrimer vs. 5 h cRCA aptamer	No	ns	0.984
Unit aptamer vs. 0.5 h cRCA aptamer	No	ns	>0.9999
Unit aptamer vs. 1 h cRCA aptamer	No	ns	>0.9999
Unit aptamer vs. 2 h cRCA aptamer	No	ns	>0.9999
Unit aptamer vs. 3 h cRCA aptamer	No	ns	>0.9999
Unit aptamer vs. 5 h cRCA aptamer	No	ns	>0.9999
0.5 h cRCA aptamer vs. 1 h cRCA aptamer	No	ns	>0.9999
0.5 h cRCA aptamer vs. 2 h cRCA aptamer	No	ns	>0.9999
0.5 h cRCA aptamer vs. 3 h cRCA aptamer	No	ns	>0.9999
0.5 h cRCA aptamer vs. 5 h cRCA aptamer	No	ns	>0.9999
1 h cRCA aptamer vs. 2 h cRCA aptamer	No	ns	>0.9999
1 h cRCA aptamer vs. 3 h cRCA aptamer	No	ns	>0.9999
1 h cRCA aptamer vs. 5 h cRCA aptamer	No	ns	>0.9999
2 h cRCA aptamer vs. 3 h cRCA aptamer	No	ns	>0.9999
2 h cRCA aptamer vs. 5 h cRCA aptamer	No	ns	>0.9999
3 h cRCA aptamer vs. 5 h cRCA aptamer	No	ns	>0.9999
0.05 mL/h			
PAMAM dendrimer vs. Unit aptamer	No	ns	0.1634
PAMAM dendrimer vs. 0.5 h cRCA aptamer	No	ns	0.0547
PAMAM dendrimer vs. 1 h cRCA aptamer	Yes	**	0.0081
PAMAM dendrimer vs. 2 h cRCA aptamer	Yes	**	0.0034
PAMAM dendrimer vs. 3 h cRCA aptamer	Yes	*	0.0102
PAMAM dendrimer vs. 5 h cRCA aptamer	Yes	*	0.0117
Unit aptamer vs. 0.5 h cRCA aptamer	No	ns	0.9986
Unit aptamer vs. 1 h cRCA aptamer	No	ns	0.8632
Unit aptamer vs. 2 h cRCA aptamer	No	ns	0.6941
Unit aptamer vs. 3 h cRCA aptamer	No	ns	0.8986

Unit aptamer vs. 5 h cRCA aptamer	No	ns	0.9161
0.5 h cRCA aptamer vs. 1 h cRCA aptamer	No	ns	0.9876
0.5 h cRCA aptamer vs. 2 h cRCA aptamer	No	ns	0.9316
0.5 h cRCA aptamer vs. 3 h cRCA aptamer	No	ns	0.9936
0.5 h cRCA aptamer vs. 5 h cRCA aptamer	No	ns	0.9958
1 h cRCA aptamer vs. 2 h cRCA aptamer	No	ns	>0.9999
1 h cRCA aptamer vs. 3 h cRCA aptamer	No	ns	>0.9999
1 h cRCA aptamer vs. 5 h cRCA aptamer	No	ns	>0.9999
2 h cRCA aptamer vs. 3 h cRCA aptamer	No	ns	0.9996
2 h cRCA aptamer vs. 5 h cRCA aptamer	No	ns	0.9992
3 h cRCA aptamer vs. 5 h cRCA aptamer	No	ns	>0.9999
0.1 mL/h			
PAMAM dendrimer vs. Unit aptamer	No	ns	0.0531
PAMAM dendrimer vs. 0.5 h cRCA aptamer	Yes	**	0.0036
PAMAM dendrimer vs. 1 h cRCA aptamer	Yes	****	<0.0001
PAMAM dendrimer vs. 2 h cRCA aptamer	Yes	****	<0.0001
PAMAM dendrimer vs. 3 h cRCA aptamer	Yes	****	<0.0001
PAMAM dendrimer vs. 5 h cRCA aptamer	Yes	****	<0.0001
Unit aptamer vs. 0.5 h cRCA aptamer	No	ns	0.942
Unit aptamer vs. 1 h cRCA aptamer	Yes	*	0.0169
Unit aptamer vs. 2 h cRCA aptamer	Yes	***	0.0008
Unit aptamer vs. 3 h cRCA aptamer	Yes	**	0.0036
Unit aptamer vs. 5 h cRCA aptamer	Yes	**	0.0055
0.5 h cRCA aptamer vs. 1 h cRCA aptamer	No	ns	0.1803
0.5 h cRCA aptamer vs. 2 h cRCA aptamer	Yes	*	0.0146
0.5 h cRCA aptamer vs. 3 h cRCA aptamer	No	ns	0.0531
0.5 h cRCA aptamer vs. 5 h cRCA aptamer	No	ns	0.0753
1 h cRCA aptamer vs. 2 h cRCA aptamer	No	ns	0.9261
1 h cRCA aptamer vs. 3 h cRCA aptamer	No	ns	0.9972
1 h cRCA aptamer vs. 5 h cRCA aptamer	No	ns	0.9995
2 h cRCA aptamer vs. 3 h cRCA aptamer	No	ns	0.9984
2 h cRCA aptamer vs. 5 h cRCA aptamer	No	ns	0.9933
3 h cRCA aptamer vs. 5 h cRCA aptamer	No	ns	>0.9999
0.5 mL/h			
PAMAM dendrimer vs. Unit aptamer	Yes	***	0.0003
PAMAM dendrimer vs. 0.5 h cRCA aptamer	Yes	****	<0.0001
PAMAM dendrimer vs. 1 h cRCA aptamer	Yes	****	<0.0001
PAMAM dendrimer vs. 2 h cRCA aptamer	Yes	****	<0.0001
PAMAM dendrimer vs. 3 h cRCA aptamer	Yes	****	<0.0001
PAMAM dendrimer vs. 5 h cRCA aptamer	Yes	****	<0.0001
Unit aptamer vs. 0.5 h cRCA aptamer	Yes	****	<0.0001
Unit aptamer vs. 1 h cRCA aptamer	Yes	****	<0.0001

Unit aptamer vs. 2 h cRCA aptamer	Yes	****	<0.0001
Unit aptamer vs. 3 h cRCA aptamer	Yes	****	<0.0001
Unit aptamer vs. 5 h cRCA aptamer	Yes	****	<0.0001
0.5 h cRCA aptamer vs. 1 h cRCA aptamer	No	ns	0.2129
0.5 h cRCA aptamer vs. 2 h cRCA aptamer	Yes	****	<0.0001
0.5 h cRCA aptamer vs. 3 h cRCA aptamer	Yes	****	<0.0001
0.5 h cRCA aptamer vs. 5 h cRCA aptamer	Yes	****	<0.0001
1 h cRCA aptamer vs. 2 h cRCA aptamer	Yes	****	<0.0001
1 h cRCA aptamer vs. 3 h cRCA aptamer	Yes	****	<0.0001
1 h cRCA aptamer vs. 5 h cRCA aptamer	Yes	**	0.0011
2 h cRCA aptamer vs. 3 h cRCA aptamer	No	ns	0.1094
2 h cRCA aptamer vs. 5 h cRCA aptamer	Yes	**	0.0088
3 h cRCA aptamer vs. 5 h cRCA aptamer	No	ns	0.942
1 mL/h			
PAMAM dendrimer vs. Unit aptamer	Yes	****	<0.0001
PAMAM dendrimer vs. 0.5 h cRCA aptamer	Yes	****	<0.0001
PAMAM dendrimer vs. 1 h cRCA aptamer	Yes	****	<0.0001
PAMAM dendrimer vs. 2 h cRCA aptamer	Yes	****	<0.0001
PAMAM dendrimer vs. 3 h cRCA aptamer	Yes	****	<0.0001
PAMAM dendrimer vs. 5 h cRCA aptamer	Yes	****	<0.0001
Unit aptamer vs. 0.5 h cRCA aptamer	Yes	****	<0.0001
Unit aptamer vs. 1 h cRCA aptamer	Yes	****	<0.0001
Unit aptamer vs. 2 h cRCA aptamer	Yes	****	<0.0001
Unit aptamer vs. 3 h cRCA aptamer	Yes	****	<0.0001
Unit aptamer vs. 5 h cRCA aptamer	Yes	****	<0.0001
0.5 h cRCA aptamer vs. 1 h cRCA aptamer	No	ns	0.9994
0.5 h cRCA aptamer vs. 2 h cRCA aptamer	Yes	****	<0.0001
0.5 h cRCA aptamer vs. 3 h cRCA aptamer	Yes	**	0.0037
0.5 h cRCA aptamer vs. 5 h cRCA aptamer	No	ns	0.4131
1 h cRCA aptamer vs. 2 h cRCA aptamer	Yes	****	<0.0001
1 h cRCA aptamer vs. 3 h cRCA aptamer	Yes	*	0.0119
1 h cRCA aptamer vs. 5 h cRCA aptamer	No	ns	0.6825
2 h cRCA aptamer vs. 3 h cRCA aptamer	Yes	***	0.0006
2 h cRCA aptamer vs. 5 h cRCA aptamer	Yes	****	<0.0001
3 h cRCA aptamer vs. 5 h cRCA aptamer	No	ns	0.3768

Table S2. Two-way ANOVA test of multiple comparison of capturing efficiency affected by arbitrary two flow rates for given modified microchannels (α= 0.05), which was obtained from Graphpad software (ns means not significant).

Tukey's multiple comparisons test	Significant?	Summary	Adjusted P Value
PAMAM dendrimer			
0.01 mL/h vs. 0.05 mL/h	No	ns	>0.9999
0.01 mL/h vs. 0.1 mL/h	No	ns	>0.9999
0.01 mL/h vs. 0.5 mL/h	No	ns	0.9999
0.01 mL/h vs. 1 mL/h	No	ns	0.9995
0.05 mL/h vs. 0.1 mL/h	No	ns	>0.9999
0.05 mL/h vs. 0.5 mL/h	No	ns	>0.9999
0.05 mL/h vs. 1 mL/h	No	ns	0.9998
0.1 mL/h vs. 0.5 mL/h	No	ns	>0.9999
0.1 mL/h vs. 1 mL/h	No	ns	>0.9999
0.5 mL/h vs. 1 mL/h	No	ns	>0.9999
Unit aptamer			
0.01 mL/h vs. 0.05 mL/h	No	ns	0.2551
0.01 mL/h vs. 0.1 mL/h	No	ns	0.0888
0.01 mL/h vs. 0.5 mL/h	Yes	***	0.0005
0.01 mL/h vs. 1 mL/h	Yes	***	0.0001
0.05 mL/h vs. 0.1 mL/h	No	ns	0.9817
0.05 mL/h vs. 0.5 mL/h	No	ns	0.1044
0.05 mL/h vs. 1 mL/h	Yes	*	0.0397
0.1 mL/h vs. 0.5 mL/h	No	ns	0.2895
0.1 mL/h vs. 1 mL/h	No	ns	0.1319
0.5 mL/h vs. 1 mL/h	No	ns	0.9924
0.5 h cRCA aptamer			
0.01 mL/h vs. 0.05 mL/h	No	ns	0.103
0.01 mL/h vs. 0.1 mL/h	Yes	**	0.0077
0.01 mL/h vs. 0.5 mL/h	Yes	****	<0.0001
0.01 mL/h vs. 1 mL/h	Yes	****	<0.0001
0.05 mL/h vs. 0.1 mL/h	No	ns	0.8186
0.05 mL/h vs. 0.5 mL/h	Yes	****	<0.0001
0.05 mL/h vs. 1 mL/h	Yes	****	<0.0001
0.1 mL/h vs. 0.5 mL/h	Yes	****	<0.0001
0.1 mL/h vs. 1 mL/h	Yes	****	<0.0001
0.5 mL/h vs. 1 mL/h	No	ns	0.055
1 h cRCA aptamer			
0.01 mL/h vs. 0.05 mL/h	Yes	*	0.025
0.01 mL/h vs. 0.1 mL/h	Yes	****	<0.0001
0.01 mL/h vs. 0.5 mL/h	Yes	****	<0.0001
0.01 mL/h vs. 1 mL/h	Yes	****	<0.0001
0.05 mL/h vs. 0.1 mL/h	No	ns	0.0534
0.05 mL/h vs. 0.5 mL/h	Yes	****	<0.0001
0.05 mL/h vs. 1 mL/h	Yes	****	<0.0001
0.1 mL/h vs. 0.5 mL/h	Yes	****	<0.0001
0.1 mL/h vs. 1 mL/h	Yes	****	<0.0001

0.5 mL/h vs. 1 mL/h	Yes	***	0.0002
2 h cRCA aptamer			
0.01 mL/h vs. 0.05 mL/h	Yes	*	0.014
0.01 mL/h vs. 0.1 mL/h	Yes	****	<0.0001
0.01 mL/h vs. 0.5 mL/h	Yes	****	<0.0001
0.01 mL/h vs. 1 mL/h	Yes	****	<0.0001
0.05 mL/h vs. 0.1 mL/h	Yes	**	0.0077
0.05 mL/h vs. 0.5 mL/h	Yes	****	<0.0001
0.05 mL/h vs. 1 mL/h	Yes	****	<0.0001
0.1 mL/h vs. 0.5 mL/h	Yes	****	<0.0001
0.1 mL/h vs. 1 mL/h	Yes	****	<0.0001
0.5 mL/h vs. 1 mL/h	Yes	***	0.0003
3 h cRCA aptamer			
0.01 mL/h vs. 0.05 mL/h	Yes	*	0.0363
0.01 mL/h vs. 0.1 mL/h	Yes	****	<0.0001
0.01 mL/h vs. 0.5 mL/h	Yes	****	<0.0001
0.01 mL/h vs. 1 mL/h	Yes	****	<0.0001
0.05 mL/h vs. 0.1 mL/h	Yes	*	0.0104
0.05 mL/h vs. 0.5 mL/h	Yes	****	<0.0001
0.05 mL/h vs. 1 mL/h	Yes	****	<0.0001
0.1 mL/h vs. 0.5 mL/h	Yes	****	<0.0001
0.1 mL/h vs. 1 mL/h	Yes	****	<0.0001
0.5 mL/h vs. 1 mL/h	Yes	****	<0.0001
5 h cRCA aptamer			
0.01 mL/h vs. 0.05 mL/h	Yes	*	0.0403
0.01 mL/h vs. 0.1 mL/h	Yes	****	<0.0001
0.01 mL/h vs. 0.5 mL/h	Yes	****	<0.0001
0.01 mL/h vs. 1 mL/h	Yes	****	<0.0001
0.05 mL/h vs. 0.1 mL/h	Yes	*	0.0136
0.05 mL/h vs. 0.5 mL/h	Yes	****	<0.0001
0.05 mL/h vs. 1 mL/h	Yes	****	<0.0001
0.1 mL/h vs. 0.5 mL/h	Yes	****	<0.0001
0.1 mL/h vs. 1 mL/h	Yes	****	<0.0001
0.5 mL/h vs. 1 mL/h	Yes	****	<0.0001